8-2020

Submerged and Floating Woody Debris-Blocking Sensitivity of Labyrinth Weirs

Taylor Vaughn
Utah State University

SUBMERGED AND FLOATING WOODY DEBRIS-BLOCKING SENSITIVITY OF LABYRINTH WEIRS

by

Taylor Vaughn

A thesis submitted in partial fulfillment
of the requirements for the degree

of

MASTER OF SCIENCE

in

Civil and Environmental Engineering

Approved:

_____	_____
Brian M. Crookston, Ph.D., P.E. Major Professor	Blake P. Tullis, Ph.D. Committee Member
_____	_____
Austin Ball, M.S., S.E. Committee Member	Richard S. Inouye, Ph.D. Vice Provost for Graduate Studies

UTAH STATE UNIVERSITY
Logan, Utah

2020

ABSTRACT

Submerged and Floating Woody Debris-Blocking Sensitivity of

Labyrinth Weirs

by

Taylor Vaughn, Master of Science

Utah State University, 2020

Major Professor: Dr. Brian M. Crookston
Department: Civil and Environmental Engineering

Accumulation of floating and submerged woody debris at flow control structures can result in reduced discharge efficiency (higher upstream head for a given weir discharge). Labyrinth weirs are more prone to debris blockage than less efficient control structures due to their ability to pass large amounts of flow with relatively small heads. Labyrinth weirs also have geometric properties that are more likely to prevent debris from passing over the weir than linear weirs.

A laboratory model study was performed to evaluate the interaction between labyrinth weirs and debris sizes. The individual debris tests indicated that debris blockage probability is influenced by trunk diameter, trunk length, and upstream head.

Debris accumulation tests indicated that lower upstream reference heads led to a greater increase in upstream head than higher upstream reference heads. At lower

upstream reference heads, head increase due to debris was up to 17%, while at higher upstream reference heads, head increase due to debris was approximately 7%. The accumulation tests also showed that larger channel width corresponds with higher increase in upstream head.

Discharge rating curves were also developed for a labyrinth weir with five fabricated submerged woody debris jams. The submerged debris tests showed that both debris volume and jam geometry highly influenced a reduction to discharge capacity of labyrinth weirs. Of the five debris jams tested, they all had an average reduction to the discharge coefficient, C_d, of at least 11% with a maximum reduction to C_d of 33%. The debris jams also corresponded to an increase in upstream head of 17% for the least impactful jam to 41% for the most impactful jam at high flows.

(89 Pages)

PUBLIC ABSTRACT

Submerged and Floating Woody Debris Blocking

Sensitivity of Labyrinth Weirs

Taylor Vaughn

Accumulation of floating and submerged woody debris at flow control structures can result in reduced discharge efficiency (higher upstream head for a given weir discharge). Labyrinth weirs are more prone to debris blockage than less efficient control structures due to their ability to pass large amounts of flow with relatively small heads. Labyrinth weirs also have geometric properties that are more likely to prevent debris from passing over the weir than linear weirs.

A laboratory study was performed to evaluate the interaction between labyrinth weirs and debris sizes. The individual debris tests indicated that debris blockage probability is influenced by trunk diameter, trunk length, and upstream head.

Debris accumulation tests indicated that lower upstream reference heads led to a greater increase in upstream head than higher upstream reference heads. The accumulation tests also showed that larger channel width corresponds with higher increase in upstream head.

Discharge rating curves were also developed for a labyrinth weir with five fabricated submerged woody debris jams. The submerged debris tests showed that both debris volume and jam geometry significantly influenced a reduction to discharge capacity and an increase to upstream head of labyrinth weirs, especially at high flows.

ACKNOWLEDGMENTS

The opportunity to perform research at the Utah Water Research Laboratory has provided me so many enjoyable, stressful, and useful experiences. Without the help of so many people, I would not have been able to complete my degree and research.

First, I would like to thank Dr. Blake Tullis for piquing my interest in water engineering through his exceptional instruction of Fluid Mechanics and the many subsequent water engineering courses he taught and furthermore for providing me a position at the Utah Water Research Laboratory (UWRL). I would also like to thank Professor Austin Ball for accepting the final position of my supervisory committee under the assumption that he may not understand what is presented to him. I would also like to thank Professor Ball for his friendship and for allowing me to spend hours talking to him about anything and everything under the pretense of professional mentorship.

Next, I would like to thank Victor Vasquez and Tina McMartin of Freese and Nichols Inc. for spending time to share their expertise on the Lake Brazos labyrinth weir and providing crucial documentation for my thesis. I would like to thank all those at the UWRL who have assisted me in my research. Specifically, Kade Flake, Wyatt Lantz, and Tucker Jorgensen for their aid in installation of the physical models. Thanks to Seth Thompson for providing so much preliminary data for the arced labyrinth weirs used in both of our research as well as his continued guidance and friendship at the UWRL. And, of course, Abby Repko for laying so much of the groundwork by collecting relevant articles, cutting sticks, spending too many hours trying to make sticks neutrally buoyant with me, and cutting more sticks.

I would also like to express my gratitude to Dr. Brian Crookston for trusting me with this research. Brian as served as a wonderful advisor and friend during this process. I am very appreciative of his patience and understanding, especially during the weeks of failed attempts to make debris neutrally buoyant. I truly could not have hoped for a better advisor.

Finally, I would like to thank my wonderful partner, Madison; Maggie; and all my family that has supported me through my entire university experience. My family has shown true interest and acceptance of my endeavors at Utah State University, and I am so thankful for all their support. Maggie has provided so much relief through her lack of interest in anything apart from food, play, and cuddles. I am very thankful for my time spent with Maggie and her minute-long pure joyfulness whenever I come home. Madi has supported me through the many late nights and extremely early mornings of being gone to collect data. She has kept me motivated when research has been frustrating and has acted interested in my studies and research. I would not have been able to complete my research, coursework, or many other things in my life without her continued support and love.

- Taylor Vaughn

CONTENTS

Page

LIST OF TABLES

Table Page

LIST OF FIGURES

Figure Page

Figure Page

NOMENCLATURE

α	Sidewall angle
c	Trunk size class
C_d	Labyrinth weir discharge coefficient
C_{dr}	Reference discharge coefficient with no debris present
D	Trunk diameter
F_D	Drag force
g	Gravitational constant
H	Upstream head
H_r	Reference upstream total head prior to adding debris
l_c	Length of sidewall
L	Length of weir crest
$L_{c\text{-}cycle}$	Length of one complete cycle
m	Debris batch number
N	Number of labyrinth weir cycles
η	Porosity of submerged debris jams
P	Weir height
PAU	Pass, upstream apex approach type
PC	Pass, cross cycle approach type
PD	Pass, stuck vertically on downstream side of upstream apex
PS	Pass, sidewall approach type
PKW	Piano key weir

Q	Discharge or volumetric flow rate
Q_d	Discharge with debris present
Q_r	Reference discharge with no debris present
SAU	Stick, upstream apex approach type
SC	Stick, cross cycle approach type
SS	Stick, sidewall approach type
θ	Labyrinth weir cycle arc angle
T	Trunk length
t_w	Labyrinth weir wall thickness at crest
V	Average flow velocity
Vdt	Volume of debris remaining after final accumulation batch is introduced
w	Cycle width
W	Channel width

INTRODUCTION

Many catchments contain various types of materials that may enter rivers, lakes, and reservoirs. These materials may be comprised of natural materials such as various types of plants, bushes, trees, etc. or pollutants such as plastics. Woody debris entering rivers may be of a wide range of sizes and can create various habitat structures. Further, some stream restoration efforts mimic these natural log jams and deposits with engineered structures of large woody debris (LWD). However, woody debris may become waterlogged over time and transition from floating debris to submerged debris (Durrum 1997).

Floating and submerged woody debris may transport to and build up at hydraulic structures during flood events. Piles of such debris can block flow passage, leading to reduced discharge capacity and increasing upstream flow depths. This can be a dam safety concern: if the spillway of a dam is blocked by debris, there may not be enough discharge capacity which could result in flooding upstream, overtopping, and potentially a failure of the structure, as was the case of the Palagnedra dam in Switzerland and the Sa Teula Dam in Italy. Both dam failures caused by debris jams are detailed in "Committee on Blockage of Spillways and Outlet Works", a report written by the International Commission on Large Dams (ICOLD 2018).

One type of spillway commonly constructed to address spillway capacity deficiencies are nonlinear weirs (Crookston et al. 2019). Although a field survey of debris issues for such weir was conducted in the USA and Portugal (Crookston et al. 2015), which concluded that most nonlinear weirs routinely pass debris, it was found that debris

does get caught on the spillway crests at low flows. Thus, there is a potential for debris blockage due to their ability to pass large amounts of flow with relatively small heads compared with linear weirs. Furthermore, their geometric properties may prevent LWD from passing over the weir. Pfister et al. (2013) performed research on debris-blocking sensitivity of piano key weirs (PKWs), a type of nonlinear weir. In the current study another type of nonlinear weir, the labyrinth weir, was analyzed with respect to the potential impacts woody debris might have on discharge capacity.

A labyrinth weir is a linear weir that is folded in plan-view to increase the crest length for a given channel or spillway width (Crookston and Tullis 2013a). Labyrinth weir flow can be described using a standard weir equation (Eq. 1)

$$Q = \frac{2}{3} C_d L \sqrt{2g} H^{3/2} \tag{1}$$

where Q is discharge over the weir, C_d is an empirically determined discharge coefficient, L is the weir's crest length, H is the total head relative to the weir's crest elevation, and g is the gravitational constant. As seen in Eq. 1, the discharge (Q) is proportional to the crest length (L); therefore, as L increases for a constant Q, the total head (H) decreases. The flow depth over a labyrinth weir for a given discharge is less than that of a linear weir; therefore, there is less flow depth for floating debris to clear the crest and reduced momentum available for debris passage. This lack of momentum from flow can lead to large debris accumulation at labyrinth weirs as shown in Fig. 1.

Fig. 1. Lake Brazos labyrinth weir, Waco, Texas
(photo courtesy of Freese and Nichols, Inc.).

The effects of woody debris on spillway capacity has received some attention, yet very limited research has been performed on debris impacts specific to labyrinth weirs. This study provides new information regarding the probability of floating debris blockage, the effects of floating debris accumulation, and the impact of multiple submerged debris jams on labyrinth weirs.

LITERATURE REVIEW

There are few studies available on the effects and probability of floating debris at labyrinth weirs. There are even fewer studies of submerged woody debris in general. Many of the studies performed on debris within rivers and reservoirs consist of analysis and observation of how debris accumulates. There have been very few model studies performed on debris in a laboratory setting to determine the probability and effects of debris build up.

Floating woody debris can arrive in rivers due to many natural and unnatural events such as flooding, forest fires, and deforestation. Woody debris in rivers can accumulate in bunches along the crest of labyrinth weirs within a river, or woody debris can become waterlogged and submerged and accumulate within and upstream of labyrinth weir cycles. Both floating and submerged woody debris accumulation may cause a reduction to discharge capacity of labyrinth weirs, leading to the need for expensive woody debris removal or potential flooding during storm events.

Debris Production and Management

The U.S. Department of Transportation Federal Highway Administration (FHWA) (2005) published an article on debris control structures that outlined some of the scenarios in which debris can accumulate at bridges, the effects associated with debris build up, and the structures used to control debris. In their article they outlined factors that affect debris production. While debris production was not addressed in the current

study, it is important to know where and why debris may be introduced to a weir in order to know whether debris needs to be considered in the design process.

FHWA listed many factors that may add to the production of debris: flooding produces debris through eroding more of the flood plain than normal flows as well as providing higher discharges to transport larger debris; fires can increase debris production through increasing the magnitude of runoff and erosion of soils, which can possibly cause landslides, depositing debris into the system; logging can increase floating debris if the appropriate practices are not used to reduce debris production; and extreme events such as ice storms, debris flows, and insect infestations can drastically increase debris production (FHWA 2005).

In 2018, the International Commission on Large Dams (ICOLD) released "Committee on Blockage of Spillways and Outlet Works". In this report, ICOLD provided a literature review of debris impacts on spillways, concerns of debris accumulation, and risk considerations. They noted that current criteria for design of spillways were not adapted to risks associated with debris such as jamming, debris clogging of spillways, and other debris related issues (ICOLD 2018).

They also reviewed various case studies of dam failures caused due to debris blockage. Most notably, the Palagnedra dam in Switzerland was discussed. A large flood in August of 1978 eroded large areas of the forest and soil upstream of the dam. Over half of the watershed was afforested with a thin topsoil layer with weak resistance to erosion on the banks. An assessment of the dam failure, which caused excessive damage and the loss of 24 lives, determined that a log jam was initially created above the reservoir and as

flow increased, the jam was brought to the spillway, jamming it. The water then continued to rise and eventually overtopped the dam leading to its failure (ICOLD 2018).

Another case study observed in the ICOLD report was that of the Sa Teula Dam in Sardinia, Italy in December of 2004. In this event, a large inflow of floating debris prevented spillway gates from opening which impeded the release of floating debris. A complete blockage of the spillway openings occurred, causing the dam to overtop and fail. In both mentioned case studies, references to how these dams could have been designed to better account for debris issues were discussed (ICOLD 2018). Both case studies show the importance of including potential debris analysis when designing dams within areas prone to debris build up.

ICOLD further discussed mechanisms by which debris enters water and is transported to spillways, how drainage basins can better be assessed for debris density and potential risk, and how to evaluate flood events that can lead to debris introduction to spillways. Finally, ICOLD discussed many ways to mitigate debris issues including but not limited to watershed management, debris dams/trash booms or racks, and debris diversion structures (ICOLD 2018). While the current study did not focus on solutions to debris, but rather focused on the level of impact debris can have, mitigation was not addressed any further; however, it does serve as an important aspect of design in debris prone areas.

Manners et al. (2007) studied the structure and hydraulics of natural woody debris jams. In their study, they analyzed the effects of varying porosity of jams formed by woody debris in the Indian River located within the Hudson River watershed in New

York State. Their study involved four levels of porosity: (1) Wrapped Jam in which they covered the existing jam with plastic wrap to simulate the assumption of no porosity, (2) Natural Jam in which no adjustments were made to the existing jam, (3) Partial Jam in which all small wood (diameter < 1 cm) and organic matter deemed unstable were removed from the existing jam, and (4) Key Member in which all accumulated debris was removed from the existing jam, leaving only the key member(s) that formed the jam initially in place (Manners et al. 2007).

Since an empirical relationship for porosity was not developed, porosity of the jams was quantified based on the jam's impacts to velocity fields and influence on the drag force, F_D, which is the difference in pressure the water exerts on the jam from upstream to downstream. When the jam was wrapped (no porosity) flow was routed around the jam. As porosity was increased through removal of debris, flow began to pass directly through the jam, increasing velocity downstream, and when only the key member(s) was left in place, the downstream and upstream velocities were nearly consistent. Since frontal area remained the same during the Wrapped Jam and Natural Jam porosity levels, the difference in hydraulics of these two stages is attributed solely to porosity. When the jam was wrapped compared to the natural jam, F_D was on average ~15% greater (Manners et al. 2007). While this study did not present a method for developing an accurate representation of a natural jam, it did indicate that porosity of debris jams plays an important role in hydraulics of jams and should be considered in design if debris jams are likely.

An important aspect of the current study was to determine the best way to model submerged debris. Buxton (2010) constructed prototype logs to simulate waterlogged wood in order to measure log friction and critical flow velocities at log entrainment in an alluvial creek. While Buxton's study was focused on research unrelated to the current study, their study provided important information on submerged debris. Buxton states, waterlogged wood is composed of hardwoods denser than water; large wood that is initially less dense than water that degrades, absorbs water, and waterlogs; and mineralized or fossilized wood. All these categories of wood are denser than water, making them unable to float and are therefore submerged (Buxton 2010).

In order to model prototype submerged debris, Buxton inserted cylinder weights throughout lodgepole pine fence posts and attached dowel rods to simulate branches. Buxton's research did not indicate the intended weight or density of the prototype log.

Crookston et al. (2015) surveyed 75 labyrinth spillways in the USA and Portugal to examine the potential for debris blockages and required maintenance of labyrinth weirs. Due to the unique geometry of the labyrinth weir, branches and trees that are transported to the weir have potential for blockages during flood events, which can reduce spillway discharge capacity and increase upstream flooding. It is also assumed that debris may be more likely to collect upstream and atop of labyrinth weirs compared to linear weirs due to the reduction of flow depth and momentum per unit weir length (Crookston et al. 2015).

Their survey found that removal of debris elements was only required for less than 7% of labyrinth spillways and that 74 of 75 surveyed dam owners/operators of

labyrinth weirs in the USA and Portugal reported no significant debris accumulations or cleaning effort. The survey also found that in cases (specifically Lake Brazos Dam) where a labyrinth weir replaced a gated spillway structure, the labyrinth weir was less problematic when dealing with debris collection and management (Crookston et al. 2015). While this survey indicated that labyrinth weirs are generally self-cleaning and require little maintenance concerning debris, the survey did not acknowledge how much debris was presented to the labyrinth weirs; therefore, probability of debris passage remained uninvestigated.

The Lake Brazos Dam was especially of interest regarding this study for the high amount of both floating and submerged woody debris affecting the labyrinth weir. The City of Waco and Freese and Nichols, Inc. (FNI) provided useful documentation regarding debris at the Lake Brazos Dam. The documentation provided included an updated rating curve accounting for debris accumulation as well as a bathymetric survey performed six years following construction of the weir to determine submerged debris accumulation.

A bathymetric survey was performed in 2007 following the construction of the labyrinth weir and again in 2013 for comparison. The bathymetric survey from 2013 indicated that approximately 9,000 cubic yards of submerged debris had accumulated since the 2007 survey. The bathymetric survey is shown in Fig. 2, and Fig. 3 shows the cross section of one of the right weir cycles to show the accumulation within and upstream of the cycle compared to the 2007 cross section when the weir was constructed. “There does not appear to be much build-up inside of the cycles near the downstream

apex. Therefore, it appears the accumulations consists mainly of debris that floated to the dam, hit the upstream apexes, and subsequently sunk" (Freese and Nichols 2013).

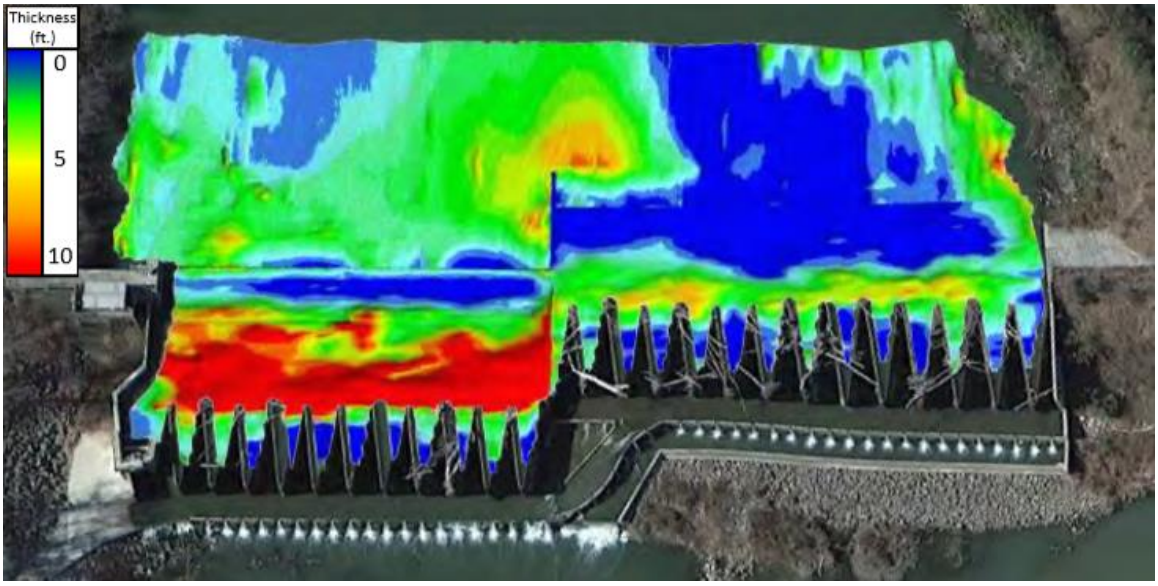

Fig. 2. Approximate Thickness of Sediment/Debris at Lake Brazos Dam (Freese and Nichols 2013).

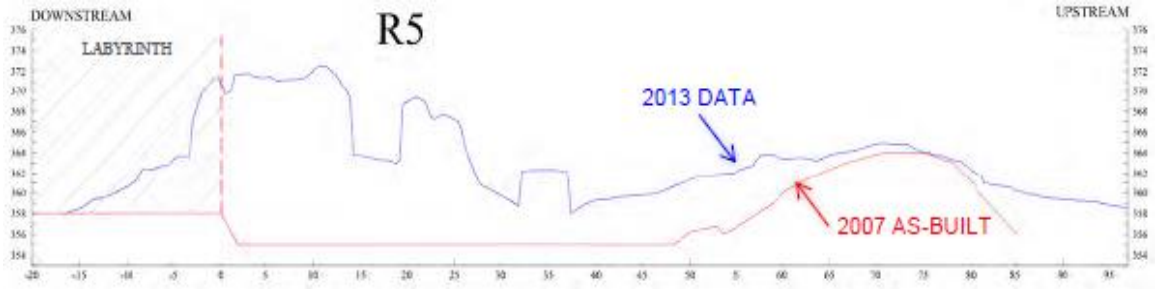

Fig. 3. Cross section of right weir cycle showing debris accumulation since construction in 2007 (Freese and Nichols 2013).

Freese and Nichols found that the greatest debris accumulation occurred just upstream of the weir and the accumulation extended at least 150 feet upstream of the dam baseline near the middle of the channel. Freese and Nichols also recommended that the City of Waco remove as much accumulated debris and sediment as possible to avoid

reduction of discharge capacity (Freese and Nichols 2013). This study did not offer any information on how the submerged debris accumulation impacted discharge capacity, but it is a very useful reference to demonstrate the possibility of extreme submerged debris accumulation.

In 2015, Freese and Nichols helped develop a new recommended rating curve for the Lake Brazos Dam to account for debris impact. By analyzing lake levels for three storm events in 2010 and one larger storm event in 2015, they noticed that the expected lake level from the rating curve developed following construction underestimated the actual lake level values found during the storms. Since construction, the weir has experienced flows up to 30,000 cfs while the 100-year flood event is anticipated to be 80,000 cfs; therefore, the recommended rating curve (shown in Fig. 4) was extrapolated from the available data to include larger storm events (Freese and Nichols 2015).

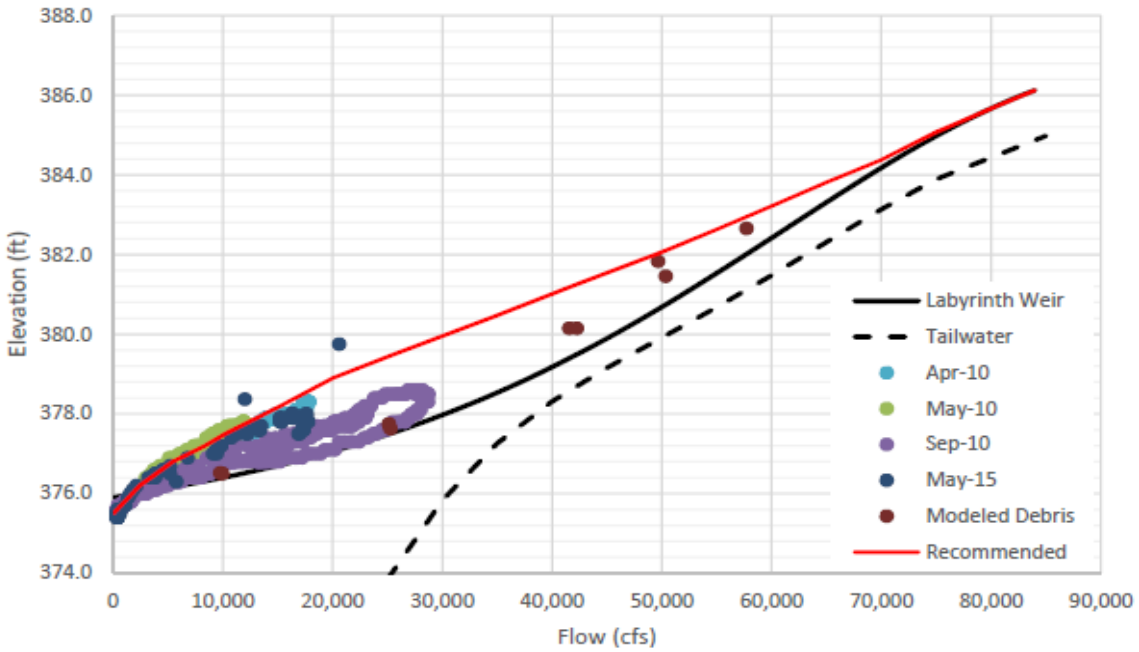

Fig. 4. Recommended rating curve for the Lake Brazos labyrinth weir accounting for debris impacts (Freese and Nichols 2015).

Freese and Nichols noted that the difference between the predicted rating curve developed during the final design of the weir and the observed recommended rating curve was likely due to the debris at the labyrinth weir. Up to two feet of additional water surface elevation is expected based on the updated rating curve (Freese and Nichols 2015). This analysis provided very relevant information regarding debris impacts on discharge capacity and served as a reference to compare results for both the floating accumulation tests and the submerged debris jam tests of the current study.

In 2003 the Utah Water Research Laboratory (UWRL) performed a preliminary design for the Lake Brazos labyrinth weir. In their physical models, the UWRL presented debris composed of shrub debris batches as well as dowel rods. Their results determined that the debris only slightly influenced flow conditions (UWRL 2003). However, their study did not use any submerged debris accumulation and the debris mats presented were very porous which may have reduced the effects of the study. As was shown by the recommended rating curve, debris accumulation had a significant impact on the actual weir. This comparison highlights that while model studies such as the current study may provide very useful information, they may be limited in their results.

The analysis provided by Freese and Nichols introduces very relevant information regarding debris impacts on discharge capacity and serves as a reference to compare for the floating debris accumulation study.

Debris Model Studies

The Bureau of Reclamation performed a model study on floating woody debris effects of a radial gated ogee crest spillway. During this study, they compared head

changes to specific gravities of debris. The study found a nonlinear relationship where the greater specific gravity of the debris produced a considerably higher impact to the results with a maximum change to head of 46 percent and a decrease in flow capacity of 43 percent at a specific gravity of 0.975 (Bureau of Reclamation 2018).

The debris was composed of 75 percent natural pieces and 25 percent dowel rods. Approximately half of the debris was soaked in water prior to testing in order to increase their specific gravity. The Bureau of Reclamation performed debris passage tests using three debris configurations: single log tests, clusters of five logs, and large complex debris mats. They used two flow rates of 50 percent and 80 percent of the dam models maximum discharge capacity. The single log tests and the log cluster tests were used to determine probability, while the debris mats were used to determine impacts to discharge capacity and water surface elevation (WSE) (Bureau of Reclamation 2018).

In addition to the jam that formed naturally at the gates, a manual compaction was performed to create an artificial debris jam to serve as a conservative upper limit to the impacts debris jams can make to the WSE and discharge capacity. The study found that for one test, during a natural jam, the test corresponded to a 2.5-foot increase in WSE and a 12.1 percent reduction in discharge capacity, while the artificial jam corresponded to a 5.3-foot increase in WSE and a 23 percent decrease in discharge capacity (Bureau of Reclamation 2018).

While the Bureau of Reclamation's study varied from the current study, there are many examples of similar procedures used in both studies. The greatest variation was the type of structure. The gated ogee crest allows for different openings allowing debris

passage to be simpler or more complicated. The gated structure also forces debris to pass underneath the structure in the water column, making debris with higher specific gravities more likely to pass (Bureau of Reclamation 2018); however, labyrinth weirs pass debris over their crest making it more likely that debris with greater specific gravities will be less likely to pass. Overall, the debris configurations were similar between the two studies with slight variations in amounts and introduction to the system. Both studies were interested in the probability of debris passage as well as impacts to discharge capacity of their respective structures.

Pfister et al. (2019) performed an experiment to determine the number of individual debris elements needed to be tested to determine a blocking probability with errors smaller than 0.09 to occur (90% confidence interval) for ogee crested weirs. By performing 14 experiments with the number of debris elements tested ranging from 20 to 70, they determined "based on the results and the statistical methods presented, it is recommended for experimental campaigns to make $n \geq 30$ repetitions per experiment so that estimations of blockage probabilities with errors smaller than 0.09 occur (with 90% confidence) (Pfister et al. 2019).

Pfister et al. (2013) performed debris studies on piano key weirs (PKWs) under reservoir approach flow to determine probability of debris blockage, debris accumulation effects, and debris volume effects. The current study was developed based on Pfister's study using labyrinth weirs and altering a few areas of the study. Pfister's study placed individual trunks with varying size classes upstream of the PKWs determining whether the trunks passed over the weir or were blocked by the weir. They also performed

accumulation tests where approximately 20 trunks of varying size classes were combined and introduced upstream of the weir. Following the introduction of debris batches, the head increase was measured to determine effects of debris accumulation (Pfister et al. 2013).

The debris for Pfister's study was classified in seven different sizes based on trunk length and diameter. It was found that trunk length had minor effect compared with trunk diameter as to whether the debris became stuck or not; therefore, the blocking probability was compared with trunk diameter over head (D/H). They found for $D/H <$ 0.33, the probability was zero apart from a few exceptions and for $D/H > 1.00$, the probability was one, indicating when $D > H$ the trunks would always become stuck. The probability increased as H decreased (Pfister et al. 2013).

The accumulation debris tests showed that for complete blocking (probability of 0.8 to 1.0) observed at small heads, the relative head significantly increases up to 1.7 times greater than the reference head. The study also found that the first trunks only slightly increased the relative head and a complete blocking of most elements is required to significantly affect H_r, where H_r is the reference upstream head. The study showed that at high heads with low probability ($H_r/P > 0.2$), the head increase for five trunks introduced compared to 10 trunks introduced were nearly identical. This would suggest that the addition of more floating debris will have little effect on the weir's discharge efficiency for $H_r/P > 0.2$ (Pfister 2013); however, Pfister did not acknowledge whether the five extra trunks added were blocked or passed. It is possible that the lack of head increase is due to the trunks passing over the weir at these higher heads, so they could not

have an impact on head. It is also possible that the additional five trunks accumulated upstream of the weir on the previous trunks rather than along the weir crest.

Supplemental research to Pfister's study of debris impacts to PKWs was performed by Pascal Venetz in 2014. In this study, during the accumulation tests, an analysis of the probability of debris blockage based on number of debris elements introduced was performed (Venetz 2014).

This analysis showed that as flow rates increased, the blocking probability of debris generally decreased indicating that head increase would be reduced due to lack of debris actually blocking the weir. The analysis also indicated that as more debris was introduced; the blocking probability of subsequent debris introduced increased. This was likely due to debris building up further upstream of the debris that initially blocked the weir (Venetz 2014).

Another useful analysis for the current study from Venetz was performed. This study showed the flow rate required for a 5% blocking probability where only 5% or less of the debris introduced was blocked by the weir and for a 95% blocking probability where 95% or more of the debris introduced was blocked by the weir. The stick class size ranged from sizes 1 through 9 where the larger class sizes indicated the larger debris elements. The smaller class sizes required a much lower flow to cause the 5% blockage probability than the larger class sizes. Furthermore, the 95% blockage probabilities only occurred for low flows (0-0.02 m^3/s) (Venetz 2014). These observations are fairly intuitive but serve as good indications of how important both flow rate and debris size are in determining whether debris will block the weir or pass over top.

Pfister and Venetz established a basis for the current study; however, there were a few modifications made. Most notably, the current study incorporated the analysis of submerged debris. There were also some aspects of the probability tests and accumulation tests that were altered from Pfister's study in the current study.

To further the research and understanding of how floating and submerged woody debris can impact labyrinth weirs, a model study was performed. The study researched labyrinth weirs regarding the probability of floating woody debris blockage based on debris size and flow, the effects of floating woody debris accumulation, and the effects of submerged woody debris accumulation.

EXPERIMENTAL SETUP

The physical modeling of the study involved installing and collecting data on three arced labyrinth weirs under reservoir type flow conditions and one traditional (non-arced) labyrinth weir in a flume. This section discusses testing facilities, weir installation processes, and instrumentation used for data collection.

Testing Facilities

The physical modeling for the three arced labyrinth weirs tested in this study was performed at the Utah Water Research Laboratory (UWRL) at Utah State University in Logan, UT (https://uwrl.usu.edu/) in an elevated, steel headbox/reservoir (7.2 m x 7.2 m x 1.5 m deep) as shown in Fig. 5. The weirs were installed, projecting into the reservoir, on an elevated (8.89 cm) acrylic platform/apron (2.75 m x 1.21 m) level to ±1.6 mm. Approach ramps sloped up from the reservoir floor at 0.073 m/m to the weir apron (Thompson 2019).

The headbox was supplied with water from an adjacent reservoir via gravity flow through a 15.2 cm (6 in.) or 50.8 cm (20 in.) diameter supply line depending on the required discharge. The headbox was elevated to allow these supply lines to enter from beneath the headbox. Water was then channeled through a diffuser pipe within the plenum chamber, which was separated from the reservoir by a baffle wall; this chamber lined three sides of the headbox to allow for reservoir-type, uniform flow conditions converging from 180° (Thompson 2019).

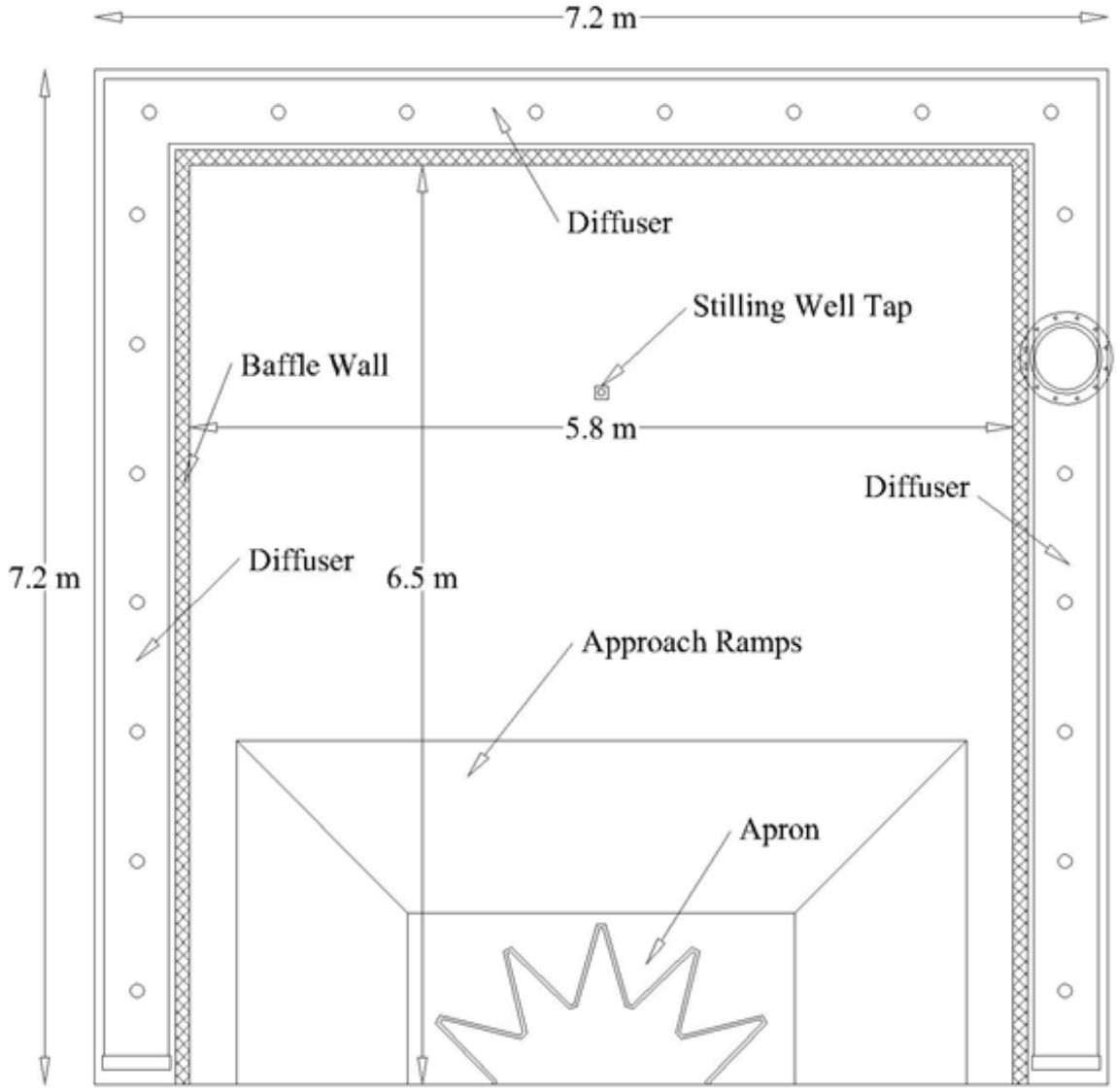

Fig. 5. Plan view of reservoir headbox with diffuser, baffle wall, stilling well tap, apron, and approach ramp labels (Thompson 2019).

Physical Models

In this study, debris tests were performed on four labyrinth weirs. Three arced labyrinth weirs with reservoir type approach flow and one labyrinth weir with river type approach flow were used as physical models. Crookston (2010) established a nomenclature for arced labyrinth weirs. Geometric parameters of arced labyrinth weirs

are presented in Fig. 6, and geometric parameters of labyrinth weirs are presented in Fig. 7; this nomenclature will be used throughout this study.

The three arced labyrinth weir models were made of polyvinyl chloride (PVC) sheeting with a weir wall height (P) of 20 cm and a nominal wall thickness (t_w), of 2.54 cm. The three arced weirs each had α = 16°, N = 5, and θ = 10°, 20°, and 30° as shown in Fig. 8. The dimensions for all three arced labyrinth weirs including entire crest length (L), channel width (W), cycle crest length ($L_{c\text{-}cycle}$), cycle width (w), cycle length to cycle width ratio ($L_{c\text{-}cycle}/w$), and cycle width to weir height ratio (w/P) are presented in Table 1 (Thompson 2019).

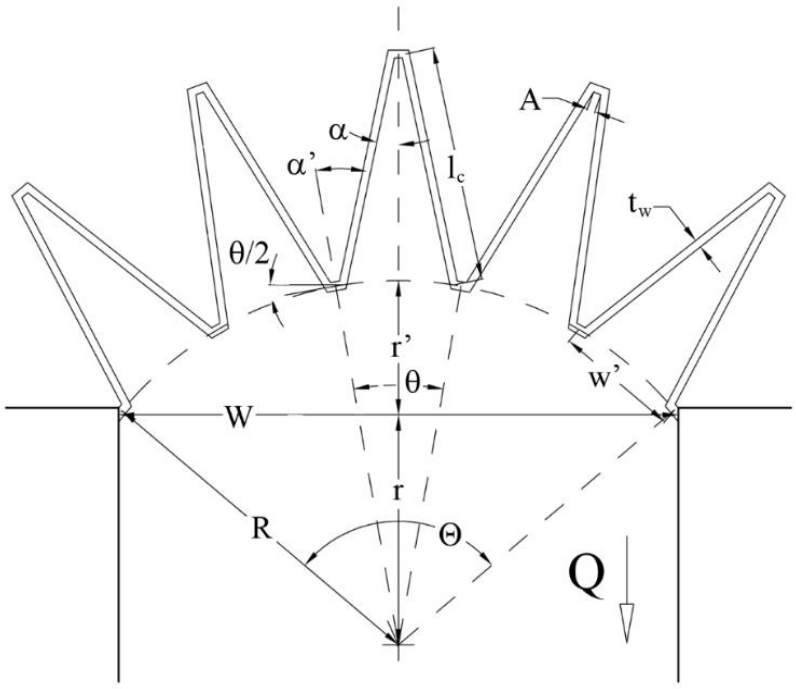

Fig. 6. Arced labyrinth weir geometric parameters (Crookston 2010).

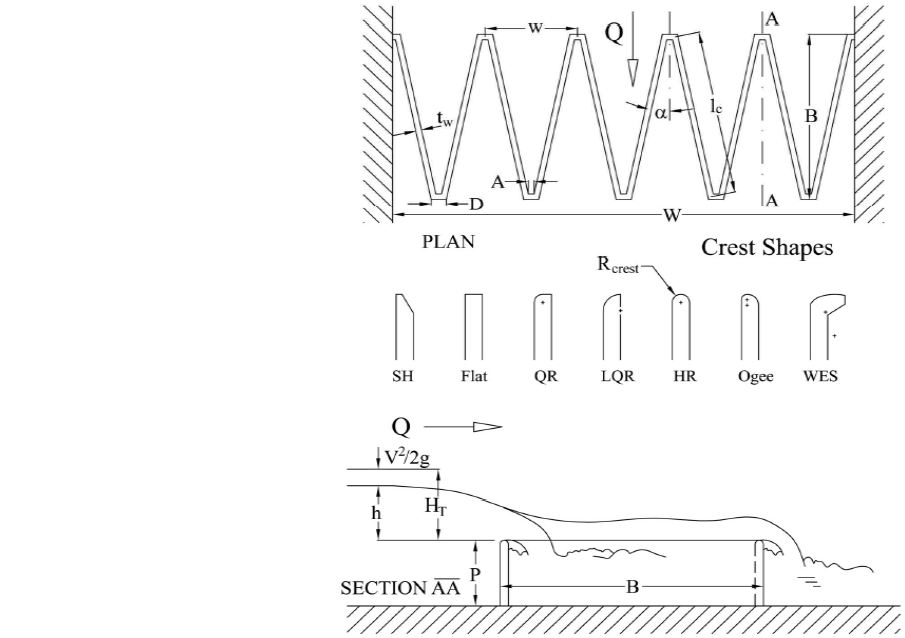

Fig. 7. Labyrinth weir geometric parameters (Crookston and Tullis 2013).

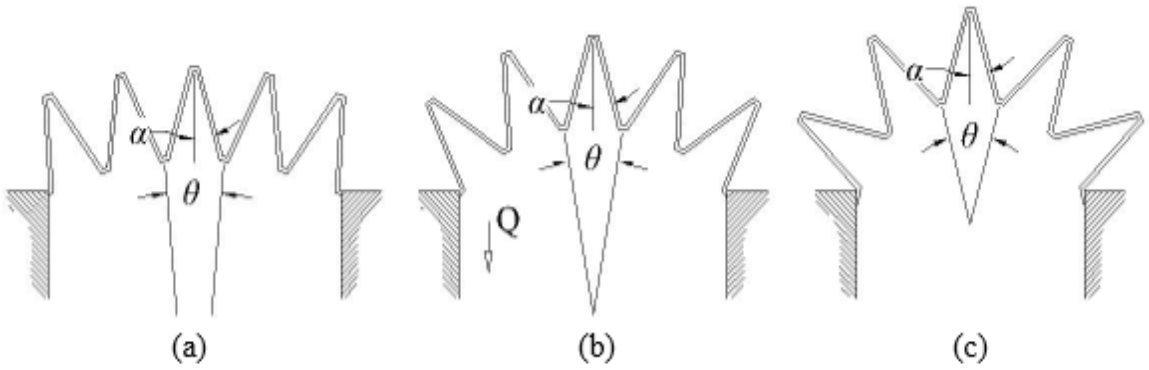

Fig. 8. Arced labyrinth weirs: α = 16° and θ = 10° (a), 20° (b), and 30° (c) (Thompson 2019).

Table 1– Arced labyrinth weir model dimensions.

Designed Dimensions									
Model	α	θ	P	L	W	$L_{c\text{-}cycle}$	w	$L_{c\text{-}cycle}/w$	w/P
	[°]	[°]	[cm]	[m]	[m]	[m]	[cm]	[cm/cm]	[cm/cm]
1	16	10	20.32	6.246	1.989	1.247	40.58	3.073	1.997
2	16	20	20.32	6.274	1.819	1.249	40.36	3.095	1.986
3	16	30	20.32	6.284	1.547	1.252	40.14	3.119	1.975

The flume weir experiments were conducted in a horizontal rectangular flume 1.2-m wide, 0.9-m deep, and 14.6-m long with an upstream baffle wall and floating wave suppressor to obtain uniform approach flow conditions. Pressure transducers connected to calibrated orifice plates were used to measure flow rate (±0.25%). A precision point gauge, readable to ± 0.15 mm, was used to measure upstream water levels in a stilling well hydraulically connected to the flume side wall, approximately 1.0 m upstream from the weir. The labyrinth weir was also made of PVC sheeting with the number of cycles (N) = 2, P = 30.5 cm, and t_w = 3.81 cm. The dimensions for the non-arced labyrinth weir are presented in Table 2, and a photo showing the weir in the flume is shown in Fig. 9.

Table 2 – Labyrinth weir model dimensions.

Designed Dimensions									
α	P	L	W	$L_{c\text{-}cycle}$	w	$L_{c\text{-}cycle}/w$	w/P	B	D
[°]	[cm]	[m]	[m]	[m]	[cm]	[cm/cm]	[cm/cm]	[m]	[cm]
10	30.48	5.758	1.224	1.372	61.19	2.242	2.008	1.389	9.97

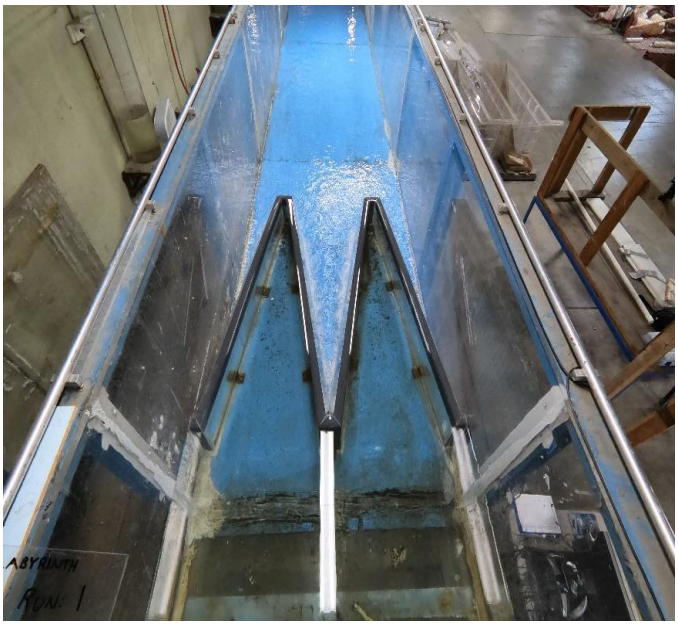

Fig. 9. Labyrinth weir in flume from upstream.

Instrumentation

Each arced labyrinth weir experiments' supply line utilized a calibrated electromagnetic flow meter (6- and 20-inch diameter ABB MagMaster® flow meters) with an average uncertainty of ±0.25% (see Fig. 10). Multimeters were connected to each flow meter to record the meters' output frequency in Hz. This reading was then converted into a discharge using each meters' calibration data. For one data point a 5 min average discharge was measured twice and recorded; if the two 5 min averages differed, another average was measured until steady state was present (Thompson 2019).

Fig. 10. 15.2 cm (a) and 50.8 cm (b) diameter supply lines with butterfly control valves (1), flow meters (2), and multimeter (3) (Thompson 2019).

To measure piezometric head, a stilling basin was hydraulically connected to the headbox and equipped with a precision point gauge (accurate within ± 0.152 mm). The piezometer in the reservoir was located at the center of the weir installation (center of middle cycle's upstream apex) and 4.89 m upstream from the downstream edge of the headbox (Thompson 2019).

Debris

To allow for comparison between the floating debris tests of labyrinth weirs in this study to the floating debris tests of piano key weirs in Pfister's (2013) study, similar trunk sizes were used. The trunks were sorted into six size classes, as presented in Table 3 and Fig. 11, where T = trunk length and D = trunk diameter. Table 3 gives the minimum, maximum, and average length and diameter of each trunk class. The average length and diameter of each size class was used to determine results. For each size class, 40 trunks were used during the floating debris tests, combining for a total of 240 data points for each flow at each weir. Trunks smaller than the size 6 trunks were initially included to test; however, due to all the trunks passing over the weirs for the lowest flow tested, they were removed from the study to save time.

The trunks used in this study were limited to individual debris segments with no rootstocks available. While this was not representative of all systems, it did represent systems where debris introduced does not include any roots of a tree. Some examples of such a system include areas where debris is introduced due to deforestation or steep slope systems where landslides can lead to broken trees for debris production. More research would need to be done to better represent systems where complete erosion of trees with roots is the primary cause of debris introduction.

Table 3 – Trunk dimensions by size class.

Size Class	1	2	3	4	5	6
Min T (m)	0.3937	0.3588	0.2921	0.2223	0.1619	0.1461
Max T (m)	0.4747	0.4509	0.3556	0.2445	0.2286	0.2096
Avg T (m)	0.4374	0.3879	0.3091	0.2326	0.1822	0.1721
Min D (m)	0.0183	0.0126	0.0094	0.0085	0.0070	0.0034
Max D (m)	0.0270	0.0184	0.0174	0.0140	0.0114	0.0076
Avg D (m)	0.0208	0.0151	0.0135	0.0109	0.0091	0.0059

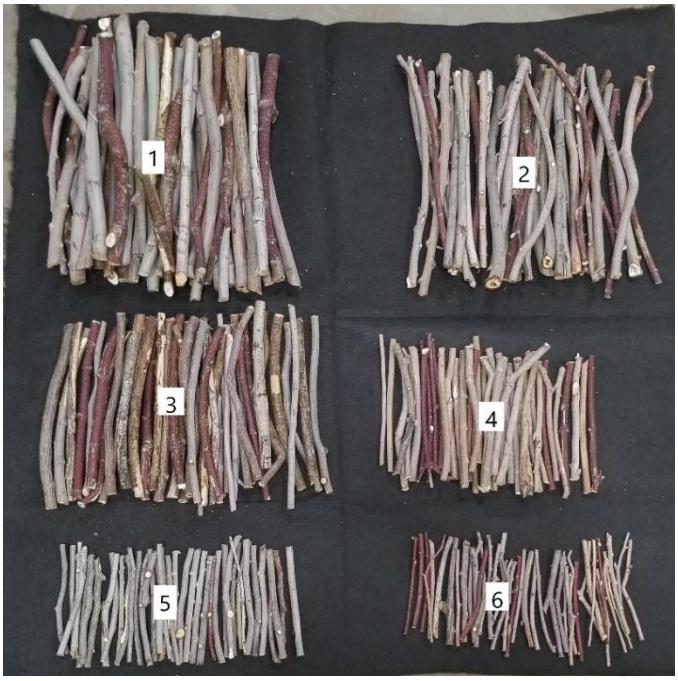

Fig. 11. Trunks by size class.

METHODOLOGY

There are two focuses for this study regarding debris impacts to labyrinth weirs: floating debris impacts and submerged debris impacts. As described by the Lake Brazos bathymetric survey and updated rating curve articles outlined in the literature review section, both floating and submerged woody debris can negatively impact labyrinth weirs.

Blocking Probability

For all four weirs, at discharge conditions ranging from total head of 0.009 meters to 0.030 meters, 40 individual trunks of every size class (see Table 3) were introduced approximately 3 meters upstream of the weir. The individual trunks were introduced at three locations across the width of the flume and five locations across the width of the headbox to ensure weir location was unbiased on whether debris was stuck or not. The result of whether each individual trunk became blocked by the weir crest (see Fig. 12) or passed over the crest was noted as well as how the trunk arrived at the crest. If a trunk was blocked by the crest it was removed before the next trunk was introduced upstream from the same location, intentionally avoiding debris accumulation.

Fig. 12. Individual trunk blocking probability test showing three stuck trunks.

Debris Accumulation

Ten debris batches consisting of 13-26 individual trunks of varying size classes were added approximately 3 meters upstream of the weirs. The volume of debris was determined and made consistent based on weir length (0.00109 m^3/m) by slightly changing the amount of debris elements in certain batches. Table 4 shows the batch size characteristics for the accumulation test in the flume. The corresponding tables for the arced labyrinth weirs can be found in Tables 1A, 2A, and 3A in Appendix A.

The 10 debris batches were introduced sequentially at the three locations across the width of the flume and five locations across the width of the headbox for each flow rate that varied between H_r of 0.009 meters to 0.030 meters where H_r is the reference upstream head prior to adding any debris batches. Five minutes after each debris batch arrived at the weir, H was recorded. Without removing any of the stuck debris elements, subsequent debris batches were introduced in the same way; this process was repeated for all 10

Table 4 – Debris batch size characteristics for flume accumulation test.

Batch number *m*	Number of trunks, Size class *c* 1	2	3	4	5	6	Elements per batch	Volume per batch (10^{-3} m^3)	Volume per batch per weir length (10^{-3} m^3/m)
1	1	1	5	2	4	3	16	0.51	0.09
2	3	1	4	2	6	1	17	0.75	0.13
3	2	4	4	6	4	3	23	0.77	0.13
4	2	3	5	4	3	2	19	0.78	0.14
5	3	1	3	4	6	3	20	0.76	0.14
6	2	2	4	3	2	3	16	0.65	0.13
7	0	4	2	2	6	0	14	0.42	0.11
8	1	1	5	3	3	3	16	0.52	0.07
9	2	1	3	5	2	0	13	0.58	0.09
10	1	3	4	1	4	2	15	0.55	0.10
TOTAL	17	21	39	32	40	20	169	6.29	1.09

debris batches. For each of the four flow rates, the effect on *H* of adding each debris batch was measured for each weir providing 40 values of *H* for each weir for a total of 160 data points for the accumulation tests.

Submerged Debris Study

The submerged debris tests consisted of developing discharge rating curves of multiple artificial debris jams of varying geometries and total debris volumes and comparing these rating curves to the rating curve of the weir with no debris present. These tests showed how much submerged woody debris build up can reduce discharge capacity.

Based upon field observations at Brazos Dam, five different debris jam scenarios were created at the labyrinth weir located in the rectangular laboratory flume using the

debris elements from the floating debris tests as illustrated in Fig. 13. As shown, the hatched areas represent these submerged debris jams. Discharge coefficients to gain insight into hydraulic efficiency were determined for the labyrinth weir with no debris present and for all five debris jams. The discharge coefficient (C_d) was computed via Eq. 1 for each datapoint. C_d data were collected for $0.05 \leq H/P \leq 0.65$.

The jams were created using the same debris elements from the floating debris tests, steel angle irons and plates to keep the debris submerged, and netting to hold the debris elements together. The volume of debris of each jam was determined by measuring dimensions of each element (woody debris elements and steel angle irons and plates) and determining their total volume. The porosity of each debris jam was then calculated by subtracting the debris volume from the jam volume determined through measurements of the boundaries of the jams.

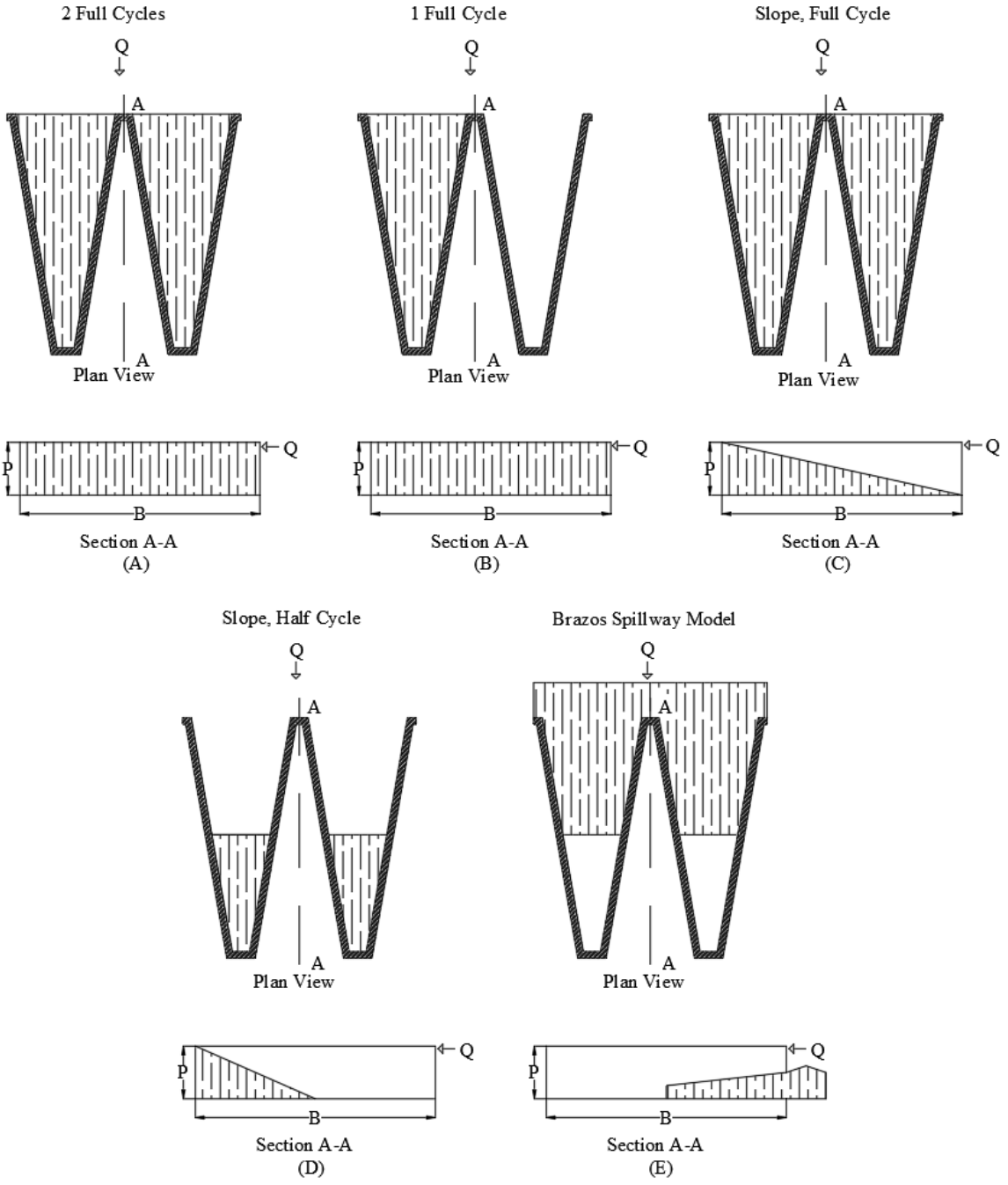

Fig. 13. Schematics of submerged debris jams: (A) 2 Full Cycles; (B) 1 Full Cycle; (C) Slope, Full Cycle; (D) Slope, Half Cycle; and (E) Brazos Spillway Model.

RESULTS

The results included in this section cover all the floating debris tests as well as the results of the submerged debris tests. Of these results, figures of the data are presented while the observed data values for the blocking probability tests can be found in Appendix B and the observed data values for the submerged debris tests can be found in Appendix C.

Blocking Probability

The analysis of the individual trunk blocking probability tests determined that *T,* *D,* and *H* had a substantial influence on blocking probability (*Π*). Blocking probability in this study is defined as the ratio of trapped debris elements to the number of supplied debris elements.

Trunk length, *T,* influenced *Π* as shown in Fig. 14. Fig. 14 shows that blocking probability is high (i.e., $\Pi \approx 1$) when $T/H \geq 35$, and blocking probability is low (i.e., $\Pi \approx 0$) when $T/H \leq 10$. For intermediate *T/H,* blocking probability can be approximated as

$$\Pi = 0.04(T/H) - 0.30 \qquad \text{for } 10 < T/H < 35 \tag{2}$$

When determining *Π* of an individual debris element on labyrinth weirs, the relationship provided through the analysis of Fig. 15 for *D/H* can also be useful. Blocking probability is high (i.e., $\Pi \approx 1$) when $D/H \geq 1.4$, and blocking probability is low (i.e., $\Pi \approx 0$) when $D/H \leq 0.4$. For intermediate *D/H,* blocking probability can be approximated as

$$\Pi = 1.05(D/H) - 0.42 \qquad \text{for } 0.4 < D/H < 1.4 \tag{3}$$

To define the manner in which debris elements arrived at the weirs, three designations were made indicating orientation and location of debris elements in

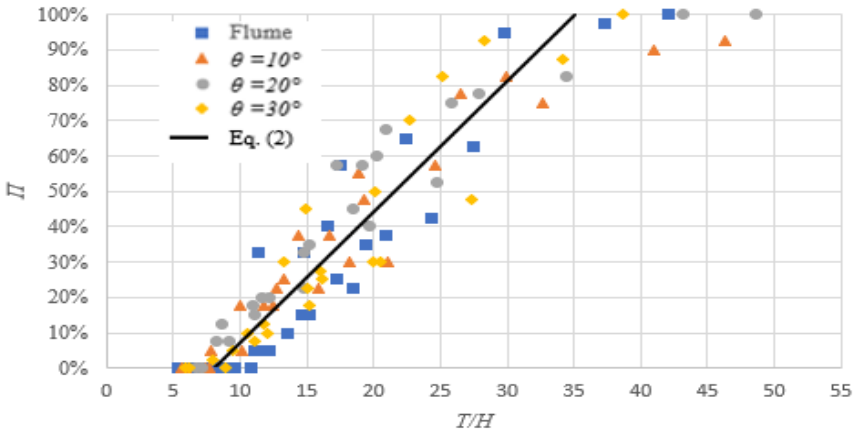

Fig. 14. Blocking probability *Π* versus *T/H*.

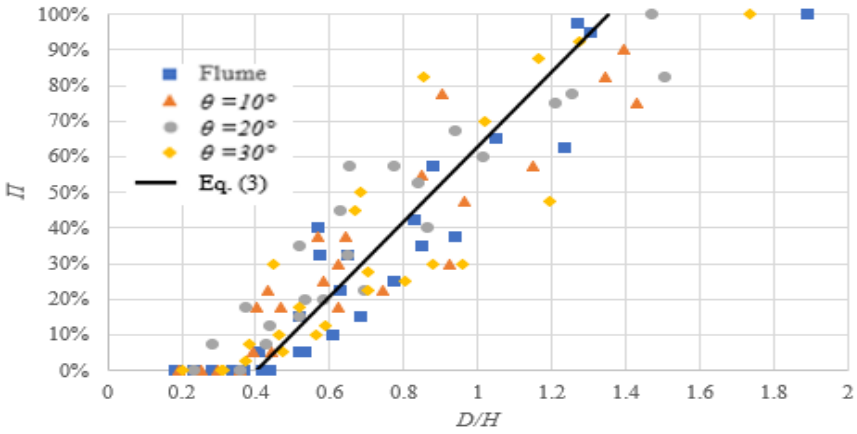

Fig. 15. Blocking probability *Π* versus *D/H*.

reference to the labyrinth weir: sidewall, cross-cycle, and apex. Examples of each of these designations are shown in Fig. 16. As shown in Fig. 17, 67% of the debris introduced approached the weir on its sidewall. The second most likely scenario was that the debris elements would approach the upstream apex of the weirs 22% of the time. Finally, debris would touch two or more cycles less than 9% of the time. The lack of likelihood that debris elements received the cross-cycle designation can be partially explained by the fact that the shorter debris elements must contact closer to the downstream apex in order to reach across a cycle.

(A)

(B)

(C)

Fig. 16. Approach type of debris elements: (A) Sidewall, (B) Apex, (C) Cross Cycle.

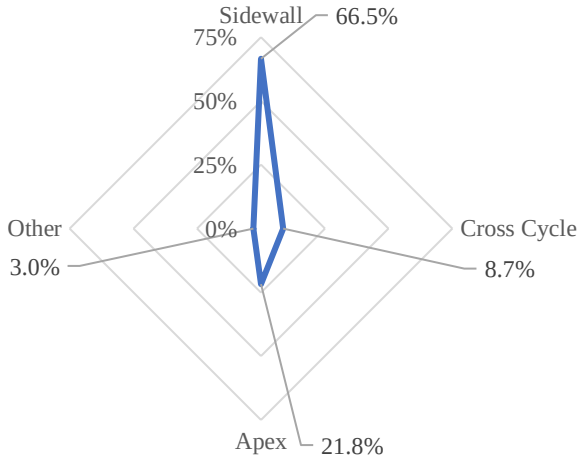

Fig. 17. Approach type of individual debris elements for blocking probability tests.

Individual debris element approach type had a direct influence on blocking probability as can be seen in Fig. 18. The most common approach type, sidewall, passed debris elements 72.8% of the time, indicating that labyrinth weirs are generally self-cleaning. When debris elements approached the weirs at the upstream apex or across two or more cycles, approximately 75% of the time debris elements were blocked by the weir. Based on these findings, orientation and location of floating debris elements as they contact the crest of labyrinth weirs significantly influenced blocking probability.

To determine the accuracy of the individual blocking probability results, an intermediate test at H of 0.015 m was run using 25 size 1 debris elements and 25 size 5 debris elements. At approximately the same flow of the original test (H = 0.015 m), 38% of the size 1 elements passed and 68% of the size 5 elements passed. During the accuracy test, 28% of the size 1 elements passed and 60% of the size 5 elements passed. This test corresponds to approximately a ±10% error of whether a debris element will pass or not.

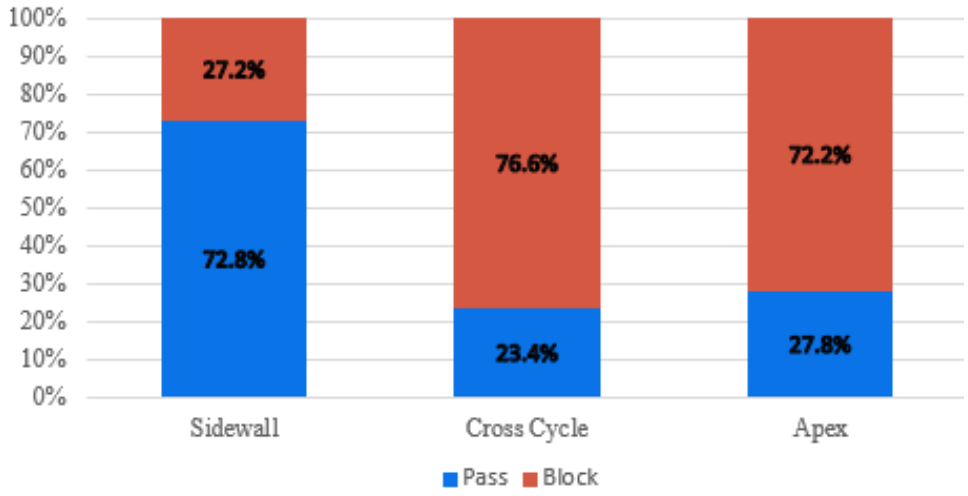

Fig. 18. Approach type blocking probability of individual debris elements.

Debris Accumulation

The accumulation effects evaluated in this study focused on the increase in upstream head due to debris. Due to the much smaller channel width, *W*, of the flume compared to the headbox weirs, H_r/P does not adequately show a useful relationship between the flume and headbox setups. This is because debris accumulates upstream of the flume weir much earlier than in the headbox as shown by the difference between Fig. 19 and Fig. 20. Fig. 19 of the flume labyrinth weir after the final batch of an accumulation test was performed shows that a small amount of debris elements touch the crest of the flume compared to Fig. 20 showing an arced labyrinth weir after the final batch of an accumulation test was performed where the majority of debris elements touched the crest. To better show the representation of head increase, H/H_r, versus reference head, H_r, the variable H_r/W is used. This relationship is represented in Fig. 21.

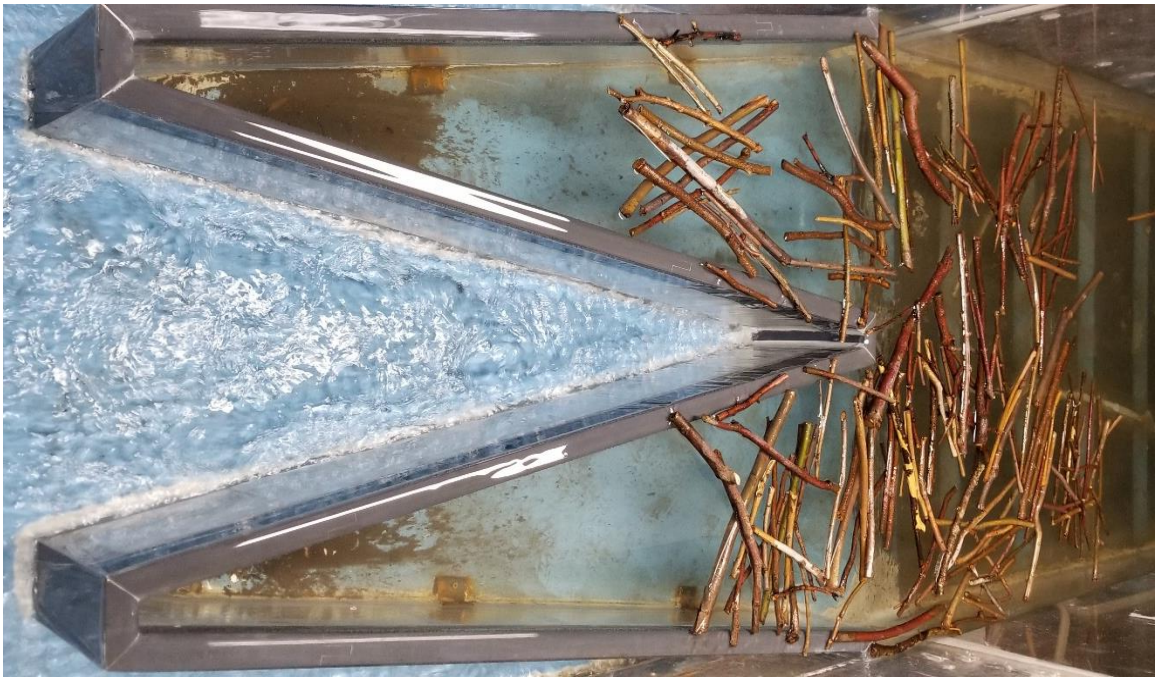

Fig. 19. Labyrinth weir debris accumulation test in flume.

Fig. 20. Arced labyrinth weir debris accumulation test in headbox.

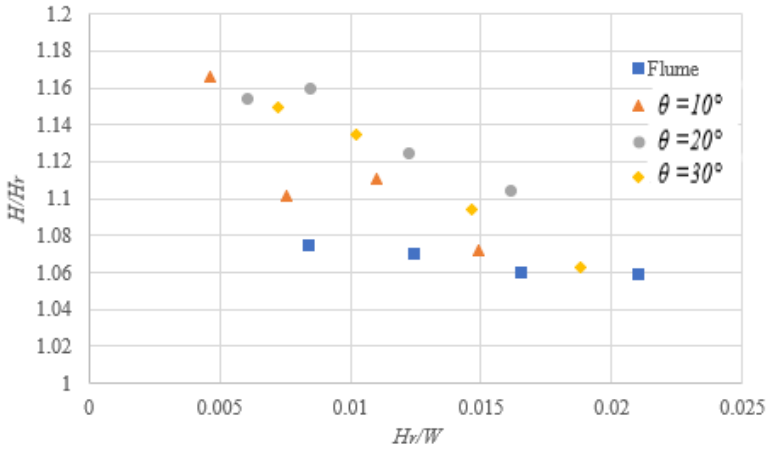

Fig. 21. Relative head increase H/H_r as a function of H_r/W.

For the four reference heads tested on the flume labyrinth weir, debris stopped approaching the crest of weir after an average of 5 debris batches with a minimum of 3 and a maximum of 9 batches. For the four reference heads tested on the arced labyrinth weirs, debris stopped approaching the crest of the weirs after an average of 8.5 debris batches with a minimum of 5 on the θ = 10° weir and a maximum of 10 (all debris approached crest) on the θ = 20° and 30° weirs. This observation helps describe the 10% difference (flume: 7% vs. arced: 17%) in reference head increase between the flume weir and the three arced weirs shown in Fig. 21.

The data indicated that low reference heads lead to a greater increase in upstream head than high reference heads. A partial explanation to this phenomenon is that at higher reference heads, debris elements were more likely to pass over the weir crest, no longer influencing upstream head. In order to further analyze how debris influenced head increase, the total amount of remaining debris accumulated at the end of the accumulation tests, not including debris that passed over the weir, were plotted versus the increase in upstream head as shown in Fig. 22.

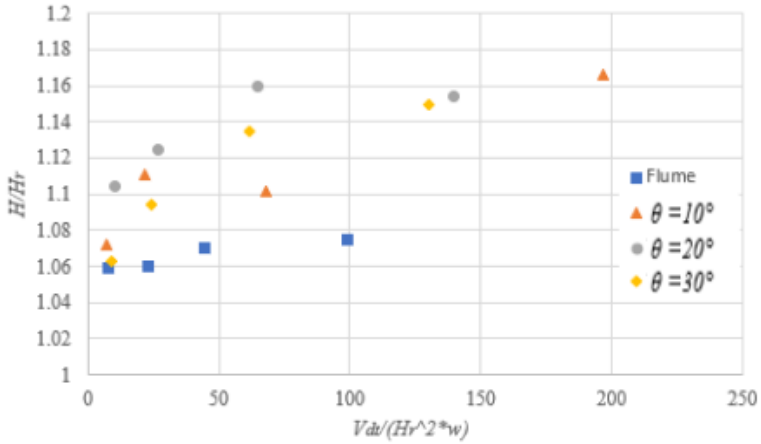

Fig. 22. Head increase versus total debris remaining at the end of accumulation tests.

By the end of most of the accumulation tests for the arced labyrinth weirs, head increase was around 17% while the flume only produced a head increase of 7%. As mentioned, this is most likely due to the smaller W of the flume than the headbox. Reference head, H_r, is lower on the high end of the x-axis of Fig. 22. This indicates that at lower heads, head increase is larger than at higher heads. V_{dt} in Fig. 22 represents the total debris remaining after the tenth and final debris batch was introduced. This parameter was used in order to avoid the effects of debris passage on the results of head increase.

While the methods used in this study should provide useful tools in design of labyrinth weirs for the likelihood and impacts of floating woody debris accumulation, it is recommended that a site-specific study be performed when designing labyrinth weirs if there are site-specific conditions not analyzed in this or other studies.

Submerged Debris

The submerged debris tests were performed by determining C_d for $0.05 \leq H/P \leq 0.65$ for the two-cycle labyrinth weir in the flume with the varying submerged debris setups

shown in Fig. 23. The results shown in Fig. 24 show the impacts that the various debris setups had on discharge capacity.

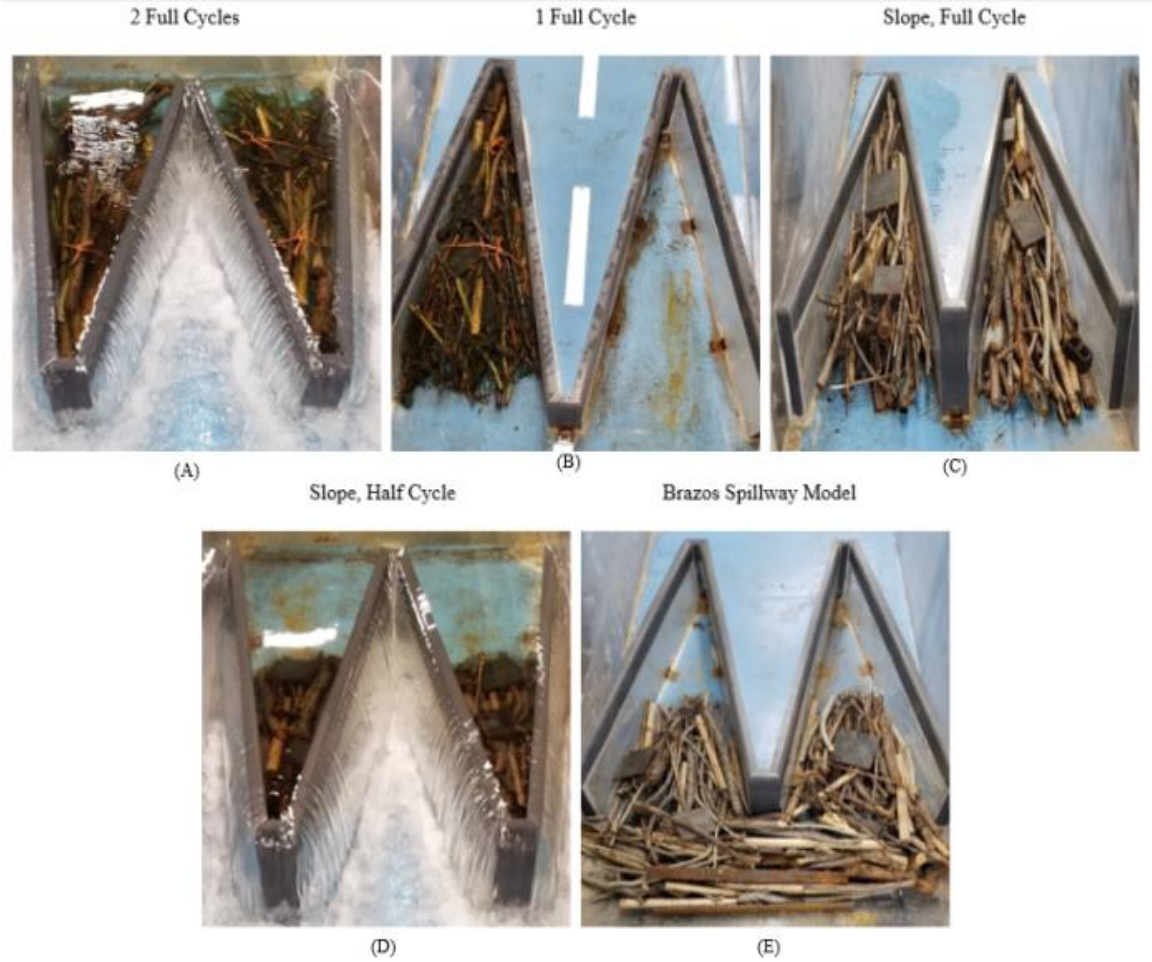

Fig. 23. Submerged debris jams: (A) 2 Full Cycles; (B) 1 Full Cycle; (C) Slope, Full Cycle; (D) Slope, Half Cycle; and (E) Brazos Spillway Model.

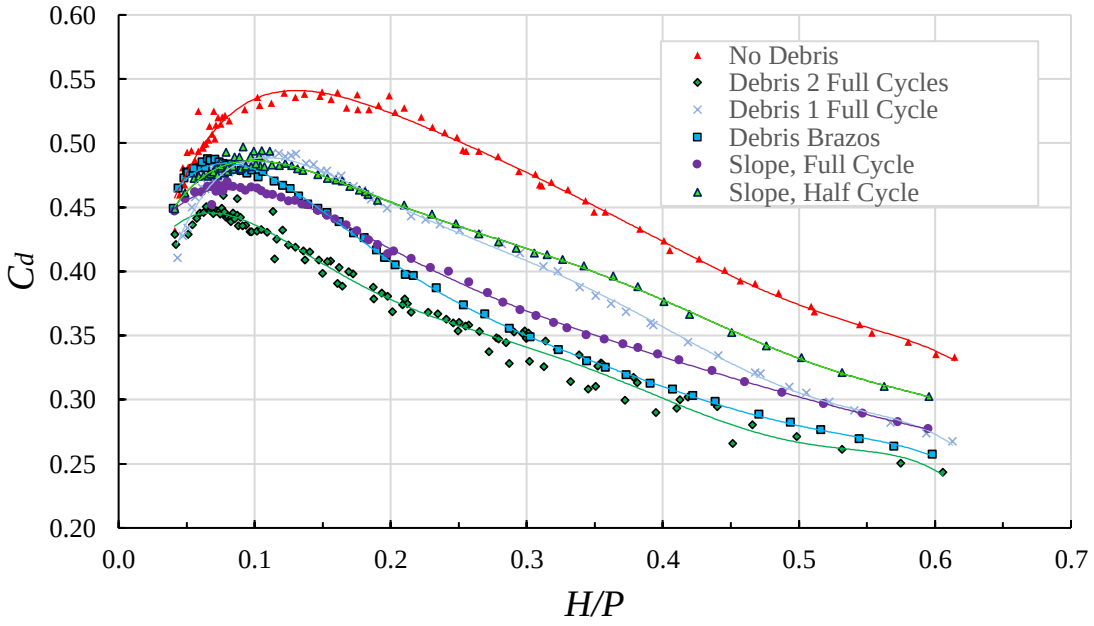

Fig. 24. C_d vs. H/P for submerged debris jams.

All submerged tests were performed in the flume weir, so all debris jam impacts are in reference to the "No Debris" setup shown in Fig. 24. The Brazos; 2 Full Cycles; and Slope, Full Cycle all had the same amount of debris present. However, all three of the setups have varying porosities (see Fig. 25) and geometries. As shown in Fig. 24, these three setups had a range of impacts on C_d: the 2 Full Cycles setup had the greatest impact. While at low flows, Brazos and Slope, Full Cycle had similar effects, but at flows of $H/P \geq 0.2$, the Brazos setup reduced C_d much more, nearing the level of 2 Full Cycles. An explanation for why the 2 Full Cycles setup had a much more extreme effect compared with setups comprised of the same volume of woody debris present is likely due to more debris near the crest of the weir affecting the water surface.

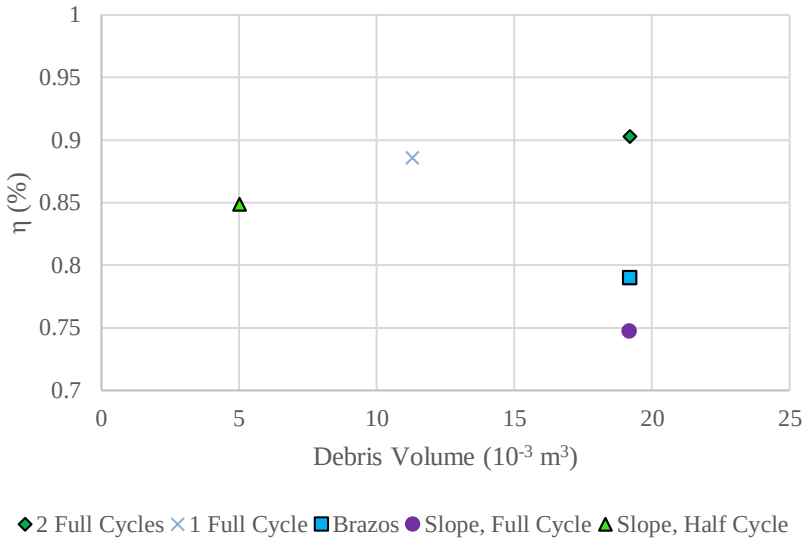

Fig. 25. Submerged debris jams volume versus porosity.

One of the most indicative ways to show just how much submerged debris can impact labyrinth weir efficiency is showing the reduction to C_d as a percent. Fig. 26 represents the reduction to C_d for every submerged debris jam. As shown, the maximum reduction (for the 2 Full Cycles setup) was 32.5% with an average reduction of 26.6%. The least affected debris jam (Slope, Half Cycle) had a maximum C_d reduction of 15% and an average reduction of 10.9%. The only model based off field data, Brazos, was also important to note as it may indicate the most likely scenario as to how submerged debris could accumulate. The Brazos setup had a maximum C_d reduction of 26.9% and an average reduction of 21.2%.

Another important observation from Fig. 26 was that C_d reduction was relatively low at low flows; however, reduction increased rapidly between H/P of 0.05 and 0.2 at which point reduction generally became constant. Since the greatest reductions will be experienced at high flows, this phenomenon could lead to serious problems during large

storm events increasing the likelihood for flooding or dam failure if submerged debris accumulates at labyrinth spillways.

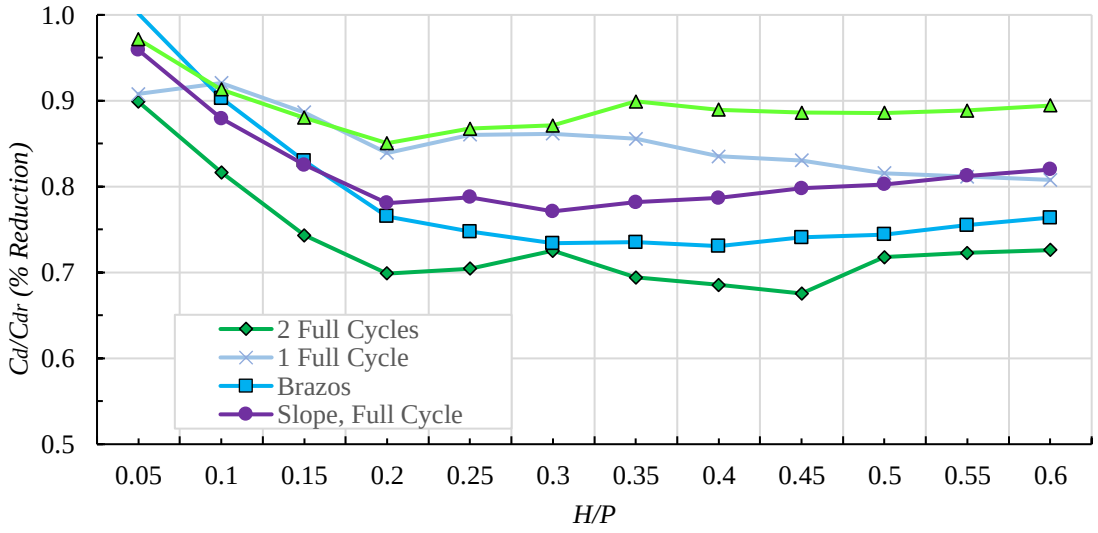

Fig. 26. C_d reduction (%) versus H/P for all debris jams.

Fig. 27 shows the reduction to flowrate over the weirs. Q_d represents the flow with debris present, while Q_r represents the reference flow when debris is not present. The top line is a one-to-one linear relationship of no debris flow for reference. The following three lines represent flow reductions of 10%, 20%, and 30%. The interpolated flow data points are then shown within the figure to represent the reduction of every submerged debris jam. All these jams led to a reduction between ~10% and ~30%.

Upstream head increase was also observed for each jam (see Fig. 28). This is another representation showing how each jam impacted flow capacity. It does prove useful when comparing to the floating debris accumulation affects. The submerged debris had between 17%-41% increase to upstream head at high flows. The floating accumulation tests had between 7%-17% increase. The results indicate that submerged debris

accumulation had a much greater impact on discharge capacity of labyrinth weirs than floating debris accumulation.

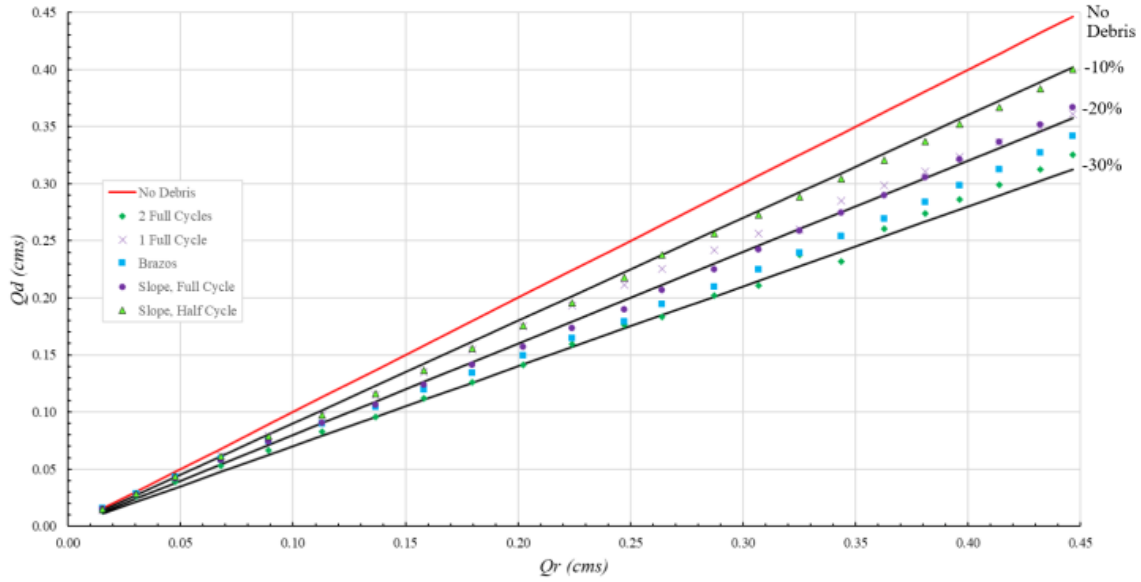

Fig. 27. Reduction to flow rate due to all submerged debris setups with 10%, 20%, and 30% reduction references.

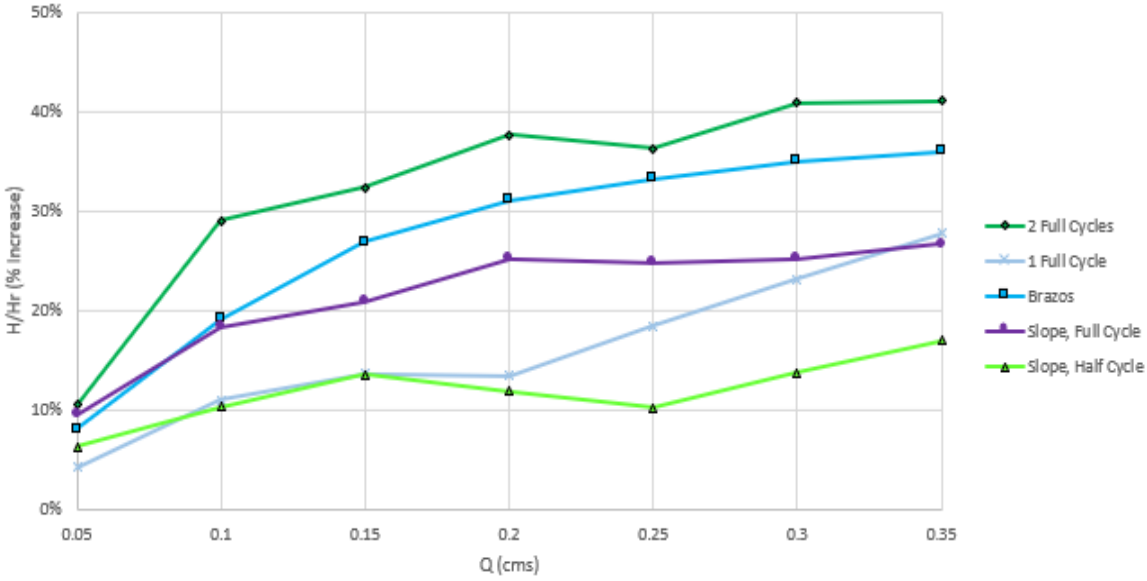

Fig. 28. Head increase for each submerged debris jam based on flow rate.

When comparing porosity alone to C_d reduction (see Fig. 29), it would appear that there is little correlation or that more porosity leads to a greater impact. The 2 Full Cycles setup had the greatest impact and the greatest porosity. This does not consider the size, amount of debris, and composition of the jam. The 2 Full Cycles setup takes up the majority of the weir cycles and disrupts the water surface more than the rest of the setups.

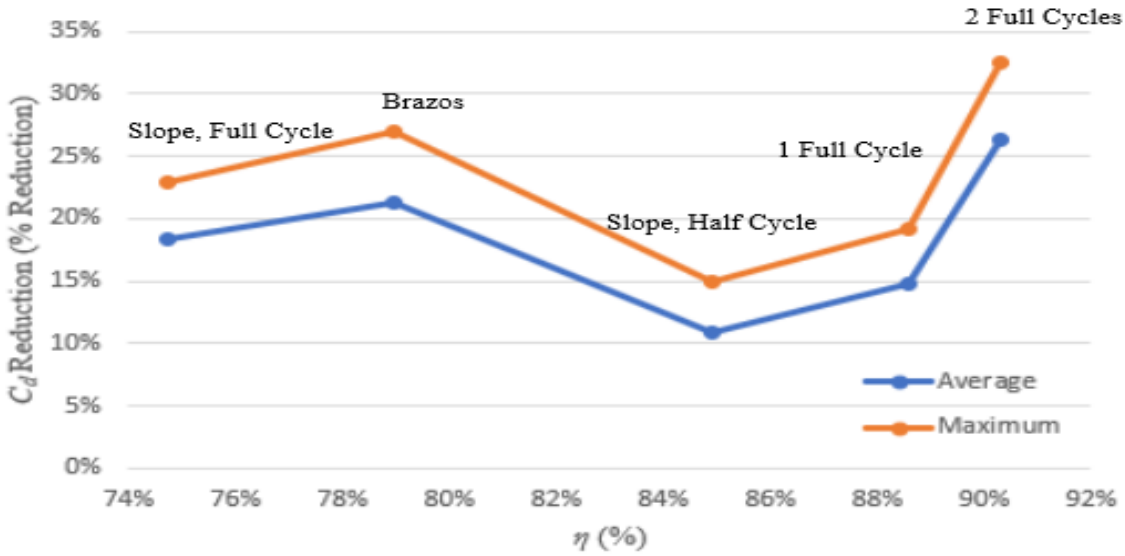

Fig. 29. Porosity of jams versus C_d reduction.

A more accurate representation of how jam porosity impacts discharge capacity was analyzed in Fig. 30. The percent of the weir's cycles' flow volume that is obstructed by the debris jam is shown in comparison to the average and maximum C_d reduction for each jam. As can be seen, the greater flow volume that was obstructed by the jam, the greater reduction to C_d was observed. The one exception was the 1 Full Cycle setup has a slightly lower reduction while it takes up more weir cycle volume than the Brazos setup. The Brazos setup is less porous and has a more complex geometry with peaks and slopes that could have led to a greater impact to the water surface. The analyses from these figures

indicates that it was more important how large the debris jams were than how porous they were.

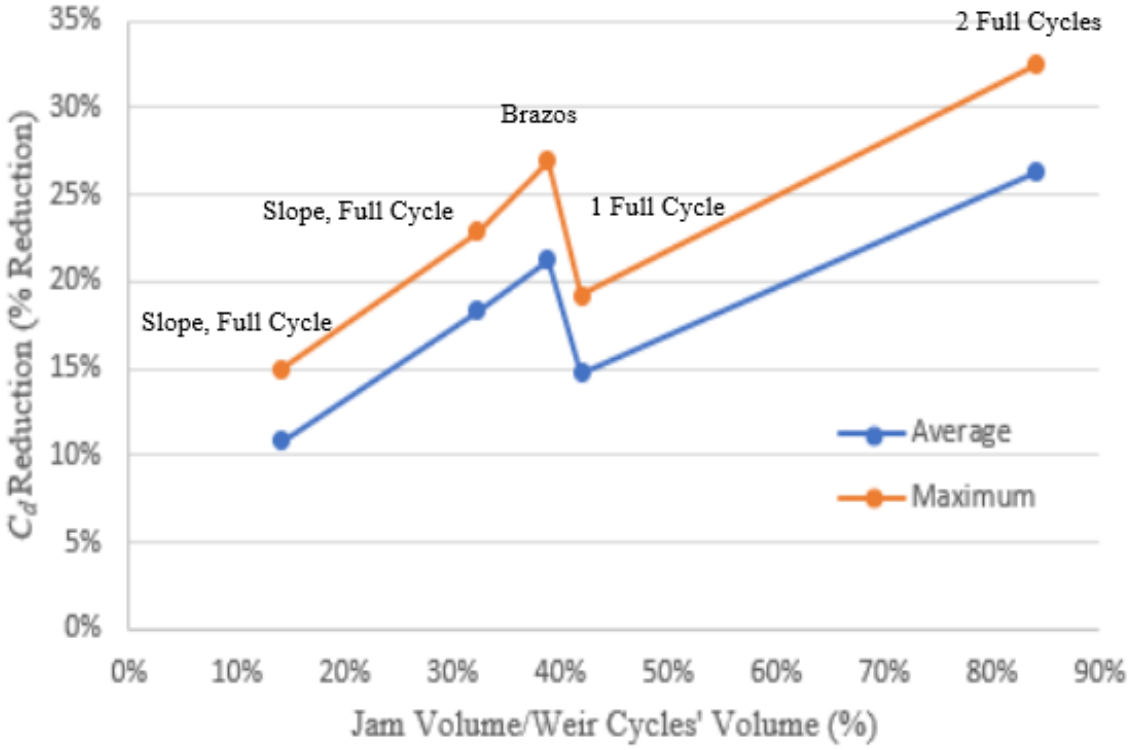

Fig. 30. Discharge coefficient reduction by obstructed weir cycle flow volume.

The results obtained from the submerged debris tests, while a good representation of how debris can negatively impact labyrinth weir discharge efficiency, may not be indicative of the types of submerged debris jams that naturally take place since only the Brazos setup was based on field data of debris accumulation. Therefore, the results should not be considered as actual representation of actual impacts, but rather, as a cautionary reference when designing labyrinth weirs in locations prone to woody debris. When designing labyrinth weirs, it is recommended that a study is performed including site-specific conditions and analyses outside the scope of this study. It is also recommended

that further research be performed on submerged woody debris with labyrinth weirs to determine how debris is likely to accumulate and when it should be of concern in design.

Both the floating and submerged woody debris tests in this study provide many useful conclusions about how labyrinth weirs respond to debris accumulation. Labyrinth weirs were found to have less debris accumulation issues and were easier to manage than other flow control structures (Crookston et al. 2015). However, if debris is an issue in a river system, changing the type of hydraulic structure in the system will not remove the issue, although it may help reduce the impacts associated with the debris issue.

The results clearly indicate that while floating and submerged debris accumulation negatively impact discharge capacity, submerged debris accumulation has a much greater impact. Floating debris accumulation can disrupt the water surface profile and prevent smooth flow passage over the weir; however, as was shown in the floating accumulation tests, after the initial jam is formed, the remainder of the debris accumulates upstream from the weir. Compared to the submerged accumulation tests, the floating debris accumulation does not impact much of the flow area of the labyrinth weir. The submerged debris accumulation was in the form of debris jams that took up large portions of the flow area within the labyrinth cycles.

In order to avoid serious negative impacts such as flooding or dam failure, a debris management plan should be in place for labyrinth weirs and other hydraulic structures in debris prone areas. Debris removal can become very expensive, especially for large amounts of submerged debris. To avoid the risks associated with debris accumulation at labyrinth weirs as well as the cost of extreme debris removal, such as dredging, a regular

maintenance plan is important for all hydraulic structures including labyrinth weirs. Early and regular maintenance will also reduce the amount of submerged debris accumulation since it takes time for debris to become waterlogged and submerged. Since submerged debris is so much more impactful than floating debris at labyrinth weirs, this regular maintenance could prove crucial in allowing labyrinth weirs to function properly and avoiding expensive maintenance procedures.

CONCLUSIONS

The purpose of this study was to lead to a better understanding of how likely woody debris is to accumulate and the impacts debris accumulation has on labyrinth weirs. This study draws attention to the severity of impacts associated with both floating and submerged woody debris on labyrinth weirs. Based on the results of this study, designers should take into consideration debris when designing labyrinth weirs. The following conclusions are based on the results of this study:

- The main dimensional parameters influencing the probability (Π) of debris blockage for individual trunk debris elements are trunk diameter (D), trunk length (T), and upstream head (H).
- Blockage probability was 0% ($\Pi = 0$) when $T/H \leq 10$. The blockage probability was 100% ($\Pi = 1.0$) when $D/H \geq 35$.
- Blockage probability was 0% ($\Pi = 0$) when $D/H \leq 0.4$. The blockage probability was 100% ($\Pi = 1.0$) when $D/H \geq 1.4$.
- Debris introduced upstream approached the weir on the sidewall 67% of the time, on the upstream apex 22% of the time, and across two or more cycles 9% of the time.
- Approach type of debris had a significant influence on Π. Debris that approached the sidewall was blocked by the weir ~27% of the time; debris that approached either at the upstream apex or across cycles was blocked by the weir ~75% of the time.

- Debris accumulation upstream of the flume weir had little effect on H; therefore, weir width (W) influenced head increase. Greater W had higher head increase due to more debris being able to accumulate on the crest.
- For low heads ($H_r/W \leq 0.01$), debris accumulation increased H by as much as 17%. For higher heads ($0.01 \leq H_r/W \leq 0.025$), debris accumulation increased H by as low as 10%. These head increases were significantly less than the 20%-70% increases of piano key weirs observed by (Pfister et al. 2013), indicating that labyrinth weirs were less influenced by floating debris accumulation in these experiments.
- Volume of debris, jam setup, location of submerged woody debris, and jam obstruction volume all influenced discharge reduction.
- The most influential submerged debris setup (2 Full Cycles) had a maximum reduction to the discharge coefficient (C_d) of ~ 33% and an average C_d reduction of ~27%.
- Of all the submerged debris jam setups the average C_d reduction ranged from 10.9% to 26.6%, and the maximum reduction ranged from 15.0% to 32.5%.
- C_d *r*eduction increased rapidly between H/P of 0.05 and 0.2 at which point reduction generally became constant. Since the greatest reductions was experienced at high flows, serious problems could arise during large storm events.

- The submerged debris jams led to a head increase of 17%-41% at high flows. This is a much greater increase than the 7%-17% caused by the floating debris accumulation.
- The submerged debris accumulation had the most impact at high flows while the floating debris accumulation had the most impact at low flows. Since debris accumulation becomes most dangerous during large flow events, submerged debris could be considered more dangerous than floating debris.
- Submerged debris accumulation had a much more significant impact on discharge efficiency than floating debris accumulation; however, both reduced capacity and should be considered in design.

REFERENCES

Bureau of Reclamation, Walker, K. (2018). “Spillway Debris Physical Model Study.” Hydraulic Investigations and Laboratory Services Group, 86-68560. Dam Safety Office Report DSO-2018-01. Hydraulic Laboratory Report HL-2018-02.

Buxton, T. H. (2010), Modeling Entrainment of Waterlogged Large Wood in Stream Channels, *Water Resour. Res., 46,* W10537, doi:10.1029/2009WR008041.

Crookston, B. M., Erpicum, S., Tullis, B. P., Laugier, F. (2019). “Hydraulics of Labyrinth and Piano Key Weirs: 100 Years of Prototype Structures, Advancements, and Future Research Needs.” J. Hydraul. Eng. doi: 10.1061/(ASCE)HY.1943-7900.0001646

Crookston, B. M., Mortensen, D., Stanard, T., Tullis, B. P., Vasquez, V. M. (2015). “Debris and Maintenance of Labyrinth Spillways.” USSD 2015 Annual Conference.

Crookston, B. M., and Tullis, B. P. (2013a). “Hydraulic Design and Analysis of Labyrinth Weirs. I: Discharge Relationships.” J. Irrig. Drain. Eng., 139(5), 363-370. doi:10.1061/(ASCE)IR.1943.4774.0000558.

Durrum E. (1997) “The Control of Floating Debris in an Urban River.” In: Coe J.M., Rogers D.B. (eds) Marine Debris. Springer Series on Environmental Management. Springer, New York, NY. doi: 10.1007/978-1-4613-8486-1_32

Freese and Nichols Inc. (2013). “Lake Brazos Dam Survey and Site Visit.” Lake Brazos Dam – City of Waco, Texas Modification Project Bathymetric/Topographic Survey.

Freese and Nichols Inc. (2015). “Lake Brazos Dam Rating Curve.” Project WPS15122 – Brazos River Hydraulic Model Update.

Furlan, P.; Pfister, M.; Matos, J.; Conceição, A.; and Schleiss, A.J. (2019). “Experimental Repetitions and Blockage of Large Stems at Ogee Crested Spillways with Piers.” J. Hydr, Res., 57:2, 250-262. https\\doi.org\10.1080/00221686.2018.1478897.

International Commission on Large Dams (ICOLD). (2018). Committee on Hydraulics for Dams. “Blockage of Spillways and Outlet Works.” Vienna, Austria. 1st July 2018. Bulletin 58-1987.

Manners, R. B., M. W. Doyle, and M. J. Small. (2007). Structure and Hydraulics of Natural Woody Debris Jams, Water Resour. Res., 43, W06432, doi:10.1029/2006WR004910.

Pfister, M., Capobianco, D., Tullis, B., M.ASCE, and Schleiss, A. J. (2013). “Debris-Blocking Sensitivity of Piano Key Weirs under Reservoir-Type Approach Flow.” J. Hydraul. Eng., 139:1134-1141. doi:10.1061/(ASCE)HY.1943-7900.0000780.

Thompson, S. D. (2019). “Reservoir Applications of Arced Labyrinth Weirs.” M.S. Thesis. Utah State University, Logan, UT.

U.S. Department of Transportation Federal Highway Administration (FHWA). (2005). “Debris Control Structures Evaluation and Countermeasures Third Edition.” Hydraulic Engineering Circular No. 9.

Utah Water Research Laboratory (UWRL) (2003). “Lake Brazos Dam Project Preliminary Design Phase Labyrinth Weir Sectional Spillway Model Study.” Prepared for Freese and Nichols Inc. Project No. 03-TO21.

Venetz, P. (2014). “Einfluss von Schwemmholz auf die Abflusscharakteristik von Klaviertasten-Wehren.”

APPENDICES

Appendix A – Debris Batch Sizes for Arced Labyrinth Accumulation Tests.

Table A1 – Debris batch size characteristics for $\theta = 10°$ accumulation test.

	Number of trunks								
	Size class c								
Batch number m	1	2	3	4	5	6	Elements per batch	Volume per batch (10^{-3} m^3)	Volume per batch per weir length (10^{-3} m^3/m)
1	1	2	5	3	4	3	18	0.59	0.09
2	2	3	4	4	6	4	23	0.78	0.12
3	2	4	3	4	5	3	21	0.77	0.12
4	1	3	5	4	2	4	19	0.64	0.10
5	1	2	3	4	6	3	19	0.54	0.09
6	1	3	4	3	2	3	16	0.57	0.09
7	2	4	4	5	6	2	23	0.84	0.14
8	2	2	5	3	3	2	17	0.70	0.11
9	1	4	3	5	2	5	20	0.63	0.10
10	2	3	4	4	4	2	19	0.75	0.12
TOTAL	15	30	40	39	40	31	195	6.83	1.09

Table A2 - Debris batch size characteristics for $\theta = 20°$ accumulation test.

Batch number m	Number of trunks: Size class c 1	2	3	4	5	6	Elements per batch	Volume per batch (10^{-3} m^3)	Volume per batch per weir length (10^{-3} m^3/m)
1	2	2	5	2	4	3	18	0.70	0.11
2	2	3	4	4	6	4	23	0.78	0.12
3	2	4	3	4	5	3	21	0.77	0.12
4	1	3	5	4	2	4	19	0.64	0.10
5	1	2	3	4	6	3	19	0.54	0.09
6	1	2	4	3	2	3	15	0.52	0.08
7	2	4	4	5	6	3	24	0.85	0.13
8	2	2	5	3	3	3	18	0.71	0.11
9	1	4	3	5	2	3	18	0.62	0.10
10	2	3	4	4	4	2	19	0.75	0.12
TOTAL	16	29	40	38	40	31	194	6.88	1.09

Table A3 – Debris batch size characteristics for $\theta = 30°$ accumulation test.

Batch number m	Number of trunks: Size class c 1	2	3	4	5	6	Elements per batch	Volume per batch (10^{-3} m^3)	Volume per batch per weir length (10^{-3} m^3/m)
1	2	2	5	2	5	4	20	0.72	0.11
2	2	3	4	4	4	4	21	0.76	0.12
3	2	4	3	4	5	3	21	0.77	0.12
4	1	3	5	4	2	4	19	0.64	0.10
5	1	2	3	4	6	3	19	0.54	0.09
6	1	2	4	3	2	3	15	0.52	0.08
7	2	4	4	5	6	5	26	0.86	0.14
8	2	3	5	3	2	3	18	0.75	0.12
9	1	4	3	5	2	4	19	0.63	0.10
10	2	3	4	4	2	2	17	0.72	0.11
TOTAL	16	30	40	38	36	35	195	6.91	1.09

Appendix B – Blocking Probability and Approach Type Data

Table B1 – Approach type and blocking probability data for flume.

Ht = 0.0104 m						Ht = 0.0159 m						Ht = 0.0209 m						Ht = 0.0255 m						Ht = 0.0324 m					
1	2	3	4	5	6	1	2	3	4	5	6	1	2	3	4	5	6	1	2	3	4	5	6	1	2	3	4	5	6
SS	SS	SC	SAU	SC	SC	SAU	PS	PS	PS	SS	PS	PS	PAU	PS	PS	PS	PS	PC	PAU	PS	PS	PS	PS	PS	PS	PS	PS	PS	PS
SC	SS	SC	PS	PS	PAU	PD	PS	SS	PS	PAU	PS	PS	SS	PS	PS	PS	PS	PS	PD	PS	PS	PS	PS	PS	PAU	PS	PS	PS	PS
SS	SAU	SC	SS	SAU	SS	PS	SAU	SS	PS	PAU	PS	PD	PAU	PAU	PS	PS	PS	SC	PS	PS	PS	PS	PS	PS	PD	PS	PS	PS	PS
SS	SS	SC	SS	SS	SAU	SAU	SAU	PS	PS	SAU	PS	PS	PAU	SAU	PS	PS	PS	PD	SAU	PS	PS	PS	PS	PD	PAU	PS	PS	PS	PS
SS	SS	SC	SS	PS	PS	SS	SS	PD	PS	PS	PS	SAU	PS	SS	PS	PS	PS	PS	PS	PS	PS	PS	PS	PS	PAU	PS	PS	PS	PS
SS	SC	SAU	PS	SC	SC	SC	SS	SAU	PS	PS	PS	PS	SC	PS	PS	PS	PS	PC	SAU	PAU	PS	PS	PS	PAU	PS	PS	PS	PS	PS
SS	SS	SAU	SS	SS	PS	SS	PS	PS	PS	PS	PS	SC	PD	PS	PS	PS	PS	PS	PAU	PS	PS	PS	PS	PAU	PS	PS	PS	PS	PS
SS	SS	SS	SS	SS	PS	PS	SC	PS	SC	PAU	PS	SAU	PS	SC	PS	PS	PS	PS	PS	PS	PS	PS	PS	PS	PS	PS	PS	PS	PS
SAU	SS	SS	SS	PS	PS	SS	PS	SS	PS	PS	PS	PS	SAU	PS	PS	PS	PS	PD	PS	SAU	PS	PS	PS	PS	PS	PS	PS	PS	PS
SS	SS	SS	PS	PS	SAU	PS	PAU	PAU	PS	PS	PS	PAU	SC	SAU	PS	PS	PS	PS	PC	PS	PS	PS	PS	PS	PS	PS	PS	PS	PS
SC	SS	SS	PS	PS	SS	PS	SS	PS	SAU	SAU	PS	PS	PC	PS	PS	PS	PS	PS	PS	PS	PS	PS	PS	SC	PC	PS	PS	PS	PS
SS	SS	SS	PS	SS	PS	PS	PS	PD	SAU	SAU	PS	SAU	SAU	SS	PS	PS	PS	PAU	PS	PAU	PS	PS	PS	PS	PS	PS	PS	PS	PS
SS	SS	SAU	PS	PS	SAU	SS	SC	PS	PS	PS	PS	PS	PC	SS	PS	PS	PS	PAU	PAU	PS	PS	PS	PS	PS	PS	PS	PS	PS	PS
SS	SAU	SC	PS	SS	SC	PD	PD	SAU	PS	PS	PS	PS	PD	PS	PS	PS	PS	PS	SAU	PS	PS	PS	PS	SAU	PS	PS	PS	PS	PS
SS	SS	SS	SC	PS	SC	SS	PS	SS	PS	PS	PS	PD	PS	SAU	SS	PS	PS	PS	PAU	PS	PS	PS	PS	PAU	PD	PS	PS	PS	PS
SAU	SS	SS	PS	SC	PS	SS	PS	SS	PAU	PS	PS	PAU	PC	PS	PS	PS	PS	SAU	PS	PS	PS	PS	PS	PS	PAU	PS	PS	PS	PS
SS	SC	SS	PS	SAU	PS	SC	SAU	PS	PS	SAU	PAU	SS	PS	SAU	PS	PS	PS	SAU	PS	PS	PS	PS	PS	PS	PS	PS	PS	PS	PS
SS	SS	SS	SAU	SS	PS	SS	SS	SAU	PS	PS	PS	PS	PS	PS	PS	PS	PS	SS	PD	PAU	PS	PS	PS	PC	PS	PS	PS	PS	PS
SS	SS	PS	SS	PS	SAU	SS	PS	PS	PD	PS	PS	PS	PD	SC	PAU	PS	PS	PS	SAU	PS	PS	PS	PS	PD	PS	PS	PS	PS	PS
SS	SS	SS	SC	PS	PS	PAU	PD	PS	PS	PS	PS	PAU	PS	PS	PS	PS	PS	PS	PS	PS	PS	PS	PS	PS	PAU	PS	PS	PS	PS
SS	SAU	SS	SS	SAU	PS	PS	PAU	PC	SS	SS	PS	SS	PS	SS	PS	PS	PS	SAU	PS	PS	PS	PS	PS	PS	PS	PS	PS	PS	PS
SS	SS	SS	SS	SS	SAU	SS	SC	SS	PAU	PAU	PS	PC	PS	PS	PS	PS	PS	PS	PS	PS	PS	PS	PS	PS	PC	PS	PS	PS	PS
SS	PS	SS	SC	PS	SC	SAU	PD	SS	PS	PAU	PAU	SC	SS	PAU	PS	PS	PS	PS	PS	PS	PS	PS	PS	PC	PS	PS	PS	PS	PS
SC	SC	SS	SS	PS	SS	SS	PS	PS	PS	PAU	PC	PS	PS	SAU	PAU	PS	PS	PD	PS	PC	PS	PS	PS	PS	PS	PS	PS	PS	PS
SAU	SS	SS	SS	PS	PS	PS	SC	SS	PS	SAU	PS	PS	PS	PS	PC	PS	PS	SAU	PC	PS	PS	PS	PS	PS	PS	PS	PS	PS	PS
SS	SS	SS	PS	PS	SS	SC	PS	PS	PS	PS	PS	SAU	PAU	PS	PAU	PS	PS	PAU	PS	PAU	PS	PS	PS	PS	PAU	PS	PS	PS	PS
SS	SS	SS	SS	SAU	PAU	SS	PD	PS	PC	PS	PS	PS	PS	PS	PS	PS	PS	PAU	PS	PS	PS	PS	PS	PD	PC	PS	PS	PS	PS
SS	SS	SS	PS	SS	PS	PAU	SS	PS	PC	PS	PS	PS	SS	PD	SAU	PS	PS	SAU	PS	SAU	PS	PS	PS	PAU	PC	PS	PS	PS	PS
SC	SS	SS	SS	SS	PS	SS	SAU	PC	PS	SS	PS	SC	SS	SC	PS	PS	PS	PS	SC	PS	PS	PS	PS	PAU	PS	PS	PS	PS	PS
SS	SS	PD	SAU	SS	PS	PS	PS	PS	PS	SS	PS	PS	PS	SAU	PS	PS	PS	SAU	PS	PS	PS	PS	PS	PS	PS	PS	PS	PS	PS
SS	SS	SS	PS	PS	PS	SS	SAU	PS	PS	PS	PS	PS	PS	PS	PS	PS	PS	PS	PS	PS	PS	PS	PS	PS	PS	PS	PS	PS	PS
SS	SS	SS	SAU	PS	PS	SS	SC	PS	PS	PS	PS	PS	PD	PC	PS	PS	PS	PC	PS	PS	PS	PS	PS	SAU	SAU	PS	PS	PS	PS
SC	SS	SS	SS	SS	SS	SS	PC	PS	PS	PS	PS	PS	PS	PS	PS	PS	PS	SS	PC	PS	PS	PS	PS	PS	PS	PS	PS	PS	PS
SS	SS	SS	SS	SS	PS	SS	PD	PS	PS	SAU	PS	PS	PS	PS	PAU	PS	PS	PS	PS	PS	PS	PS	PS	PS	PS	PS	PS	PS	PS
SS	SS	SC	SC	PS	SS	PS	SS	PC	SS	SS	PS	SC	PD	PS	PS	PS	PS	PS	PD	PS	PS	PS	PS	PS	PS	PS	PS	PS	PS
SS	SS	SS	SS	SS	PS	PS	SS	SS	PS	SAU	PS	SS	PAU	PS	PS	PS	PS	PS	PS	PS	PS	PS	PS	PAU	PC	PS	PS	PS	PS
SS	SS	SS	SC	SS	PS	SS	PS	PS	SAU	SS	PS	SC	PS	PC	PAU	PS	PS	PAU	PS	PS	PS	PS	PS	PS	SC	PS	PS	PS	PS
SC	SAU	SS	SS	PS	PS	PS	PS	PAU	PS	PS	PS	SC	PAU	PAU	PAU	PS	PS	PS	PS	PS	PS	PS	PS	SC	PS	PS	PS	PS	PS
SS	SS	SS	PS	SS	PS	SS	PS	SS	PS	PS	PS	SS	PS	PS	PS	PS	PS	SAU	PS	PAU	PS	PS	PS	PS	PS	PS	PS	PS	PS
SAU	SC	SS	PAU	SAU	PS	SC	PAU	SC	PAU	PC	PAU	SAU	SS	PS	PC	PS	PS	PS	SAU	PS	PS	PS	PS	PS	PS	PS	PS	PS	PS

Table B2 – Approach type and blocking probability data for $\theta = 10°$.

Ht = 0.0095 m						Ht = 0.0146 m						Ht = 0.0232 m						Ht = 0.0305 m					
1	2	3	4	5	6	1	2	3	4	5	6	1	2	3	4	5	6	1	2	3	4	5	6
SS	SC	SC	SAU	PS	PS	SC	PS	PS	SAU	PS	PS	SS	PS	PC	PAU	PS	PS	SC	PAU	PS	PS	PS	PS
SAU	SAU	SS	PS	PS	PS	SAU	SAU	PS	PS	PS	PS	SC	PS	SAU	PAU	PS	PS	PD	SAU	PAU	PS	PS	PS
SS	SAU	SAU	PS	PAU	PS	SAU	SC	PS	SAU	PS	PS	SC	PS	SC	PAU	PAU	PS	P	PAU	PS	PS	PS	PS
SS	SS	SS	PS	SAU	PS	SAU	SAU	PS	PC	PAU	PS	PS	SAU	PS	P	SAU	PS	PS	P	PAU	PS	PS	PS
PD	SC	SAU	PD	SAU	PS	SC	PS	SAU	PS	PS	PS	SC	PAU	PAU	PS	SAU	PS	SAU	PS	PC	PS	PS	PS
SS	SS	SC	SC	SAU	PS	SC	SC	PS	PS	PS	PS	SAU	PS	SAU	PS	PAU	PS	SAU	PS	PS	PS	PS	PS
SS	SS	SAU	SC	PAU	PS	SAU	SAU	PS	PS	SAU	PS	SAU	PS	SAU	PAU	PS	PS	PS	PS	PS	PS	PS	PS
SS	SS	SAU	SC	SAU	PS	SAU	SC	SAU	PS	PAU	SAU	SC	PS	PAU	SS	PS	PS	PAU	PS	PAU	PS	PS	PS
SS	PD	SAU	PD	PS	PS	SAU	SS	SAU	PAU	PS	PS	SAU	PS	PS	PS	PS	PS	PAU	PS	PS	PS	PS	PS
SC	SC	PS	SS	SAU	SAU	SAU	SAU	PS	PS	PS	PS	PAU	SAU	PS	PS	PS	PS	SS	PS	PS	PS	PS	PS
SS	SS	PD	PS	PS	SAU	SS	SAU	PS	PS	PS	S	PC	PS	PS	PS	PAU	PS	SAU	SAU	PS	PS	PS	PS
SS	SAU	SS	SS	SAU	PS	SC	SAU	PAU	SC	SAU	SS	SC	PS	PS	PS	PAU	PS	SC	PD	PS	PS	PS	PS
SS	SS	SAU	PS	SAU	PS	SAU	PS	SAU	PS	SAU	PS	SAU	PS	PS	PS	PS	PS	PS	PS	SAU	PS	PS	PS
SC	SS	SC	PS	PS	SAU	SAU	SC	S	SAU	PS	PS	PS	SAU	SAU	PS	PS	PS	SAU	SAU	PS	PS	PS	PS
SAU	SS	SAU	SS	SAU	SAU	SS	SAU	SS	PS	PS	PS	SC	SAU	PS	PS	PS	PS	PS	PS	PS	PS	PS	PS
SS	SAU	PS	SS	PS	SAU	PS	PS	PS	PS	PS	PS	PS	SS	PS	PS	PS	PS	PS	PS	PS	PS	PS	PS
SC	SS	SS	PS	PS	PS	SS	SAU	PAU	SS	PS	PS	PAU	PS	PS	SAU	PS	PS	PS	PS	PS	PS	PS	PS
SS	SAU	PS	PS	PS	PAU	SC	PC	PS	PS	PS	PS	PS	PS	PC	PS	PS	PS	SAU	PC	PS	PS	PS	PS
SS	SC	PS	SAU	PS	PS	PS	PS	SAU	PS	PS	PS	PS	SC	PS	PS	PS	PS	PC	SC	PS	PS	PS	PS
PAU	SC	PD	SS	PS	SS	SC	SC	PS	PAU	PS	PS	PS	SAU	PS	PS	PS	PS	PAU	PAU	PS	PS	PS	PS
SS	SS	SS	SAU	SAU	SS	SS	SS	PS	SAU	PS	PS	PS	SAU	PS	PC	PAU	PS	PC	PC	PS	PS	PS	PS
SS	PD	PS	SAU	PS	PS	SAU	SAU	PS	PS	SAU	SAU	PC	PS	PS	PS	PS	PS	SAU	PAU	PS	PS	PS	PS
SS	SS	SS	SS	SAU	SAU	SAU	SS	PS	PS	PS	PS	PS	PS	SAU	PS	PS	PS	SS	PS	PAU	PS	PS	PS
SS	SS	SAU	SS	SAU	PS	SS	SS	PS	PS	PS	SAU	SAU	SAU	PS	PS	PS	PS	PS	SAU	PS	PS	PS	PS
SC	SS	SS	SS	SC	PS	SAU	SC	PS	SAU	PS	PAU	SS	PS	PS	PS	PS	PS	PS	PAU	PS	PS	PS	PS
PS	SS	SC	PS	SS	SS	PS	SS	PS	PS	SS	PAU	SAU	SC	SAU	PS	PS	PS	PS	PC	PS	PS	PS	PS
SS	PD	PS	PD	PS	SAU	SC	SC	SAU	PAU	PS	PS	SC	SS	PS	SC	PS	PS	PS	PC	PAU	PS	PS	PS
SS	SS	SC	SAU	PS	PS	SS	SS	SS	PS	PS	PAU	PS	PS	PC	SAU	PS	PS	PS	PS	PAU	PS	PS	PS
SC	SS	SAU	SAU	SAU	PS	SC	SAU	PS	PS	PS	SAU	PS	PS	PS	PS	PS	PS	SAU	PAU	PS	PS	PS	PS
SC	SS	SAU	PS	PS	PS	PS	PS	PS	PS	PS	SAU	SC	PS	PS	PS	PAU	PS	PS	PS	PS	PS	PS	PS
SS	SS	SAU	PS	PS	PS	SS	SAU	PS	PAU	SAU	PS	SAU	PS	PS	PS	PS	PS	PS	PS	PAU	PS	PS	PS
SC	SC	SS	SS	PAU	SAU	PAU	SC	SS	PS	PS	PS	PS	SAU	PS	PS	PS	PS	PS	PAU	PS	PS	PS	PS
SS	SS	SAU	PS	SAU	PS	SS	SS	PS	SAU	PS	PAU	SS	PS	PS	PS	PS	PS	SAU	SAU	PS	PS	PS	PS
SS	SS	PD	SAU	SAU	PS	PS	PS	PS	PC	PS	PS	PS	SAU	PC	PS	PS	PS	PAU	SS	SAU	PS	PS	PS
SS	SC	SAU	PS	PS	PC	SAU	SAU	SAU	PS	PAU	PS	PS	PS	PAU	PS	PS	PS	PS	PS	PS	PS	PS	PS
SS	SAU	PS	SS	PS	PS	SC	SC	PS	PS	PS	PS	SS	PS	PS	SS	PAU	PS	PS	PS	PS	PS	PS	PS
SS	SAU	SS	SS	SAU	PS	SC	SAU	PS	PS	PS	PS	PS	SS	SS	PS	PS	PS	SAU	PS	PS	PS	PS	PS
SC	PD	SC	PS	SS	SS	PS	SAU	PS	PAU	S	PS	SC	PS	SAU	SS	PS	PS	PS	SAU	PS	PS	PS	PS
SS	SS	SS	SS	PS	PS	SAU	SC	SAU	SAU	PS	PS	SS	PS	PS	PS	PAU	PS	PS	PS	PS	PS	PS	PS
SS	SS	SC	SAU	SAU	PS	SC	PS	PS	PS	PS	PS	SAU	SS	PS	PS	PS	PS	SAU	PS	PS	PS	PS	PS

Table B3 - Approach type and blocking probability data for $\theta = 20°$.

Ht = 0.0090 m						Ht = 0.0157 m						Ht = 0.0209 m						Ht = 0.0255 m					
1	2	3	4	5	6	1	2	3	4	5	6	1	2	3	4	5	6	1	2	3	4	5	6
SS	SS	SS	SAU	SAU	SAU	PS	PS	SAU	PS	SS	PS	SS	PS	PC	SAU	PS	PS	SC	PAU	SAU	PS	PS	PS
SS	SC	SS	SAU	PS	PAU	SAU	PS	PS	SAU	SAU	PS	SC	PS	SAU	PAU	PS	PS	PS	SAU	PAU	PS	PS	PS
SS	SS	SS	SC	PS	SAU	PS	PD	PS	PAU	PS	PS	SC	PS	SC	SAU	PAU	PS	PS	SAU	PS	PAU	PS	PS
SC	SC	PS	PS	SAU	SAU	SAU	PS	SAU	PAU	PS	SC	PS	PAU	PS	P	PAU	PAU	SS	P	PAU	PS	PS	PS
SAU	SAU	SS	SS	PS	SS	SS	PC	SAU	PS	PS	PS	SC	SAU	SAU	PS	SAU	PAU	SAU	PS	PC	PS	PS	PS
SS	SS	PS	SAU	S	PS	SAU	SC	SAU	PD	PS	PS	SAU	PS	PAU	PS	PAU	PS	SAU	SS	PS	SAU	PS	PS
SS	SS	SS	SS	PS	PS	SAU	SS	SS	PS	PS	PS	SAU	PS	SAU	PAU	PS	PS	PS	PS	PS	PS	PS	PS
SC	SS	SS	SS	SS	PS	SS	PS	PS	PS	PS	PS	SC	PS	PAU	PS	PS	PS	SAU	PS	PAU	PAU	PS	PS
SS	SS	SAU	SS	SC	SS	SC	SAU	SAU	PS	PAU	SAU	SAU	PS	PS	PS	PS	PS	SAU	PS	S	PS	PS	PS
SS	SS	SAU	SS	SS	SAU	SAU	SS	PS	PD	SAU	PS	PAU	SAU	PS	PS	PS	PAU	SS	PS	PS	PS	PS	PS
SC	SAU	SC	SAU	PS	SC	PD	SAU	PD	PS	PS	PS	PC	PS	PS	SS	PS	PS	SAU	SAU	PS	SAU	PS	PS
SS	SS	SS	SS	PS	PS	SS	PS	PS	PS	PS	PS	SC	PS	PS	PS	PAU	PS	SC	PD	PS	PS	PS	PS
SS	SS	SS	SS	PS	SAU	SC	PD	SAU	SAU	PS	PS	SAU	PS	PS	PS	PS	SAU	SS	PS	SAU	PS	PS	PS
SC	SS	PS	SC	SS	SC	SAU	SC	PS	PS	PS	PS	PS	SAU	SAU	PS	PS	PS	SAU	SAU	PS	PS	PS	PS
SS	SS	PS	PS	SS	SS	SC	SC	PS	PD	SAU	PS	SC	SAU	PS	PS	PS	PS	PS	PS	PS	PS	PS	PS
SC	SS	SS	PD	PAU	PAU	SAU	SAU	SC	PS	SAU	SS	PS	PS	PS	PS	PAU	PAU	SS	SS	PS	SAU	PS	PS
SAU	SAU	SS	SS	SS	PS	SC	SAU	SS	SS	SS	SAU	SAU	SS	PS	SAU	PS	PS	PS	PS	PS	PS	PS	PS
SC	SC	SS	SS	SS	SS	SC	PS	PS	SAU	SS	PS	SS	SS	PC	PS	SAU	SAU	SAU	PC	PS	PS	PS	PS
SS	SS	SS	SAU	SS	SS	SAU	SAU	PS	PS	PS	PS	PS	SC	PS	PS	PS	PS	PC	SC	PS	PS	PS	PS
SC	SS	SAU	SS	SS	SC	SAU	PD	SAU	PS	PS	PS	SS	SAU	PS	PS	PS	PS	PAU	PAU	PS	PS	PS	PS
SAU	SC	SS	SC	SS	SS	SS	PD	PS	PS	PS	PS	SS	SAU	SS	PC	PAU	PS	SC	SC	PS	PS	PS	PS
SC	SC	SS	SS	SAU	PS	SS	PAU	PS	SAU	PS	PS	SC	PS	PS	PS	PS	PS	PAU	PAU	PS	PC	PS	PS
SAU	SAU	SS	SS	PS	PS	PD	SS	PS	PS	PS	SAU	PS	PS	SAU	PS	PS	PS	SS	PS	SAU	PS	PS	PS
SS	SS	PS	PS	PS	SS	SC	PS	PAU	PS	PS	SAU	SAU	SAU	PS	PS	PS	PS	SS	SAU	PS	PS	PS	PS
SAU	SS	SS	PS	PS	SS	SAU	PS	PS	SAU	PAU	PS	SS	PS	PS	PS	SAU	PS	PS	PAU	PS	PS	PS	PS
SS	SS	SS	PD	SAU	PS	SAU	PD	SC	PS	PS	PS	SAU	SC	SAU	PS	SAU	PS	PS	SC	PS	PAU	PS	PS
SS	SS	PS	SS	PS	SS	PS	SC	SAU	PS	PS	SS	SC	SS	PS	PC	PS	PS	SS	PC	SAU	PS	PS	PS
SS	SS	SS	SS	PS	SAU	SS	PS	SAU	PS	SS	PAU	PS	PS	SC	SAU	PS	PAU	PS	PS	PAU	PS	PS	PS
SS	SS	SS	PD	SS	SS	SAU	PS	PD	PS	PS	PS	PS	SS	PS	PS	PS	PS	SAU	PAU	PS	PS	PS	PS
SAU	SS	SAU	PS	SAU	PS	SAU	SC	PS	SAU	PS	PS	SC	PS	PS	PS	PAU	PS	PS	PS	PS	PS	PS	PS
SS	SS	SS	PS	SS	PS	PS	SAU	PS	PAU	PS	PS	SAU	PS	SS	PS	PS	PS	PS	PS	SAU	PAU	PS	PS
SC	SS	SAU	PS	PS	SS	SS	PS	PAU	PS	PS	PAU	PS	SAU	PS	PS	PS	SAU	PS	PAU	PS	PS	PS	PS
SAU	SAU	SS	SAU	SS	PS	SC	SC	PC	PS	PS	PS	SS	PS	PS	PS	PS	PS	SAU	SAU	PS	PS	PS	PS
SS	SS	PS	SS	SS	PS	SAU	PS	SAU	PS	PS	PS	PS	SAU	PC	PS	PS	PAU	SAU	SS	SAU	PAU	PS	PS
SS	SC	SS	SS	PS	SS	PS	SAU	SC	PC	PS	PS	PS	PS	SAU	PS	PS	PAU	PS	PS	PS	PS	PS	PS
SS	SS	SS	SS	PS	SS	SC	SAU	PD	PS	PAU	PS	SS	PS	SS	PS	SAU	PS	PS	PS	PS	PS	PS	PS
SS	SS	SS	SS	SS	PS	SAU	SS	PS	SAU	PS	PS	PS	SS	PS	PS	PS	PS	SAU	PS	SS	PS	PS	PS
SS	SS	SAU	SAU	SAU	SS	PD	SS	PS	PS	PS	PS	SC	PS	SAU	PS	PS	PS	PS	SAU	PS	PAU	PS	PS
SC	SS	SS	SS	SS	PS	PS	SC	SAU	PS	PS	PS	SS	SS	PS	PS	PAU	PS	SS	PS	PS	PS	PS	PS
SAU	SC	SS	SS	SS	PAU	SC	SC	PD	SC	PAU	PS	SAU	SS	PS	PS	PS	PS	SAU	PS	PS	PS	PS	PS

Table B4 - Approach type and blocking probability data for $\theta = 30°$.

Ht = 0.0113 m						Ht = 0.0154 m						Ht = 0.0211 m						Ht = 0.0293					
1	2	3	4	5	6	1	2	3	4	5	6	1	2	3	4	5	6	1	2	3	4	5	6
SS	SC	SS	PS	PAU	PS	SS	PS	PS	PS	PS	PS	PS	PS	PS	PS	PS	PS	PS	PS	PS	PS	PS	PS
SS	SAU	PS	PD	PS	PS	SS	SAU	SAU	PS	PS	PS	SS	PS	PS	PS	PS	PS	SS	PS	PS	PS	PS	PS
SS	SAU	PS	PS	PAU	PS	SAU	SAU	PAU	PD	PS	PS	SS	PS	PS	PS	PS	PS	PS	PD	PS	PS	PS	PS
SAU	SS	PS	PS	PS	PS	SS	SAU	PD	PS	PD	PS	SC	SS	PS	PS	PS	PS	PS	PS	PS	PD	PS	PS
SAU	SAU	SS	PS	PAU	PS	SC	SC	PS	PS	PS	PS	SS	SS	PAU	PS	PS	PS	SC	PS	PAU	PS	PS	PS
SS	SS	SAU	SAU	PS	PS	SC	PS	SS	SAU	SAU	PS	SAU	PS	SAU	PS	PS	PS	PS	PAU	PS	PS	PS	PS
SC	PD	SC	PS	SAU	PS	SAU	SAU	SAU	PS	PS	PS	PS	SS	PS	PS	PS	PS	SS	PS	PS	PS	PS	PS
SC	SS	PS	SS	PS	PS	SS	SAU	PS	PS	PS	PS	PS	SAU	PS	PS	PS	PS	SAU	PS	PS	PS	PS	PS
SS	SS	PS	SAU	PS	PS	SS	SC	PS	PS	PS	PS	SS	PS	SAU	PS	PS	PS	PS	SAU	PS	PS	PS	PS
SS	SAU	SS	PC	PS	PS	SS	SS	SAU	PS	SAU	PS	PD	SAU	PS	PS	PS	PS	PS	PS	PD	PD	PS	PS
SS	SS	PS	PS	SAU	PS	SS	SS	PS	PD	PS	PS	SS	SAU	PS	SAU	PS	PS	SS	SS	PS	PS	PS	PS
SS	SS	PD	PS	PS	SAU	PS	SS	PS	PS	PS	PS	PS	SS	PS	PS	PS	PS	SS	SAU	PS	PS	PS	PS
SC	SS	SS	PAU	SAU	PS	SS	PS	PS	PS	PS	PS	SS	PS	PS	PS	PS	PS	PS	PS	PS	PAU	PS	PS
SAU	SAU	PS	PS	PS	PD	SS	SS	SAU	PS	PS	PS	SAU	PS	PS	PS	PS	PS	SAU	SAU	PS	PS	PS	PS
SS	SS	SAU	PS	PS	PS	SAU	SS	PS	PS	PAU	PS	SC	SAU	PC	PS	PS	PS	PS	PS	PS	PS	PS	PS
SS	SS	PS	PAU	SAU	SAU	SS	SAU	PC	SAU	PS	PS	SAU	PS	PS	PC	PS	PS	PS	PS	SAU	PS	PS	PS
SAU	SS	PS	PS	SAU	PS	SS	SS	PAU	PS	PS	PS	SAU	PS	PS	PS	PS	PS	SS	SAU	PS	PS	PS	PS
SS	SAU	PS	SC	PS	PS	SAU	SAU	SAU	PS	PS	PS	SS	SS	SAU	PAU	PS	PS	PS	PS	PS	PS	PS	PS
SAU	SC	SAU	PS	PS	SAU	SAU	SAU	PS	SAU	PAU	PS	SS	PS	PAU	PS	PS	PS	SAU	PS	PS	PS	PS	PS
SS	SAU	PS	SAU	SAU	PS	SC	PS	PD	PS	PS	PS	PS	SS	SAU	PS	SAU	PS	PS	SS	PS	PS	PS	PS
SC	SC	SC	SAU	SAU	PS	SC	SS	PS	PS	SAU	SAU	SS	SS	SS	PS	PS	PS	SS	PS	PS	PS	PS	PS
SAU	SS	PS	PS	PS	SAU	PS	SC	PS	PS	PS	PS	PS	SAU	PS	PS	PS	PS	SS	PS	PS	SAU	PS	PS
SS	SS	SS	SAU	PS	PS	SAU	SC	PS	PS	PS	PS	PS	SC	PS	PS	PS	PS	SAU	PS	PS	PS	PS	PS
SS	SAU	SAU	PS	PS	PS	SS	SS	PS	PS	PS	PS	SS	PS	PS	SAU	PS	PS	PS	PS	SAU	PS	PS	PS
SS	PS	SC	PS	PS	PS	SAU	SS	SC	PS	PS	SAU	PS	SS	SS	PS	PS	PS	SAU	SAU	PS	PS	PS	PS
SS	PS	SS	PS	PS	PS	SAU	SAU	PS	PD	PS	PS	SS	SAU	PS	PS	PS	PS	PS	PS	PS	PS	PS	PS
SC	SC	PS	SAU	PS	PS	SS	SS	PS	PAU	PS	PS	SS	SAU	PS	PS	PS	PS	PS	SAU	PS	PS	PS	PS
SS	SS	PS	PS	PS	PAU	SS	SS	SAU	PS	PS	PS	SC	PS	PS	SAU	PS	PS	SAU	PS	PS	PC	PS	PS
SS	PS	SAU	PC	SAU	SAU	SS	SC	PS	SC	PS	PAU	SS	SS	PS	PS	PS	PS	PS	PS	PS	PS	PS	PS
SS	SAU	SC	SC	PS	PS	SS	PD	SS	PS	PS	PS	SC	PS	SAU	PS	PS	PS	PS	PS	SAU	PS	PS	PS
SAU	SS	PS	PS	PS	PS	SS	SS	PS	PS	SAU	PS	SAU	PS	SAU	PS	PS	PS	SS	SAU	PS	PS	PS	PS
SAU	SS	SAU	PS	PAU	PS	SC	PS	PS	PS	PS	PAU	PS	PS	PS	PS	SAU	PS	PS	PS	PS	PS	PS	PS
SAU	SS	PS	SAU	PD	PS	SS	SC	PS	SAU	PS	SAU	SS	PAU	PS	PS	PS	PS	PS	SS	PS	PAU	PS	PS
SS	SS	PD	PS	SAU	PS	SS	SS	PD	PS	PS	PS	SS	PD	SAU	PS	PS	PS	SAU	PS	PS	PS	PS	PS
SS	SS	SAU	PS	PS	PS	SS	PS	SAU	PS	PS	PS	PS	SS	PS	PS	PS	PS	PS	PS	PS	PS	PS	PS
SAU	SS	PS	PS	PS	PAU	SAU	SS	PS	SAU	SAU	PS	SS	SAU	PS	SAU	PAU	PS	SS	PS	PS	PS	PS	PS
SS	SS	SS	SS	PS	SAU	SC	SS	PAU	PS	PS	PS	PS	PS	PS	PS	PS	PS	PS	SS	PS	PS	PS	PS
SS	SAU	SS	PS	SAU	PS	SS	SAU	SS	SAU	PS	PS	SS	PS	SAU	PS	PAU	PS	PS	PS	PS	PS	PS	PS
SS	SS	PS	PS	PS	PS	PS	SS	SS	SS	PS	PS	SAU	PS	PS	PS	PS	PS	SAU	SAU	PD	PS	PS	PS
SS	PS	PD	SS	PS	SAU	SS	SS	PS	SAU	PD	PD	SAU	SS	SAU	PS	PS	PS	PS	PS	SAU	PAU	PS	PS

Appendix C – Tabulated Submerged Debris Test Results

Table C1 – No Debris submerged debris setup tabulated results.

Q [cms]	H [m]	H/P [-]	C_d [-]
0.021	0.018	0.059	0.525
0.028	0.021	0.070	0.525
0.100	0.049	0.161	0.539
0.113	0.053	0.175	0.538
0.126	0.058	0.191	0.530
0.136	0.061	0.199	0.537
0.145	0.064	0.210	0.528
0.156	0.068	0.222	0.520
0.163	0.070	0.231	0.513
0.171	0.073	0.240	0.508
0.179	0.076	0.249	0.504
0.192	0.081	0.265	0.494
0.206	0.085	0.279	0.489
0.218	0.090	0.294	0.478
0.231	0.093	0.307	0.476
0.241	0.097	0.318	0.470
0.252	0.101	0.330	0.464
0.262	0.105	0.343	0.455
0.273	0.109	0.358	0.446
0.294	0.117	0.383	0.433
0.308	0.122	0.401	0.424
0.327	0.130	0.427	0.410
0.341	0.136	0.445	0.401
0.357	0.143	0.468	0.390
0.370	0.148	0.485	0.383
0.387	0.155	0.509	0.373
0.412	0.166	0.545	0.358
0.436	0.177	0.580	0.345
0.460	0.187	0.615	0.333
0.014	0.014	0.047	0.481
0.017	0.016	0.053	0.494
0.020	0.018	0.058	0.494

0.022	0.019	0.062	0.496
0.010	0.013	0.041	0.432
0.012	0.014	0.045	0.459
0.014	0.015	0.048	0.467
0.016	0.016	0.051	0.481
0.017	0.017	0.054	0.480
0.019	0.017	0.056	0.486
0.020	0.018	0.059	0.483
0.021	0.019	0.062	0.481
0.022	0.019	0.063	0.499
0.023	0.020	0.064	0.499
0.024	0.020	0.066	0.502
0.025	0.020	0.067	0.513
0.026	0.021	0.069	0.507
0.027	0.022	0.071	0.503
0.028	0.022	0.071	0.514
0.029	0.022	0.073	0.520
0.030	0.023	0.075	0.515
0.031	0.023	0.076	0.521
0.033	0.024	0.078	0.522
0.034	0.025	0.081	0.518
0.050	0.032	0.104	0.529
0.043	0.028	0.093	0.526
0.072	0.040	0.130	0.536
0.057	0.034	0.112	0.531
0.065	0.037	0.122	0.539
0.088	0.045	0.148	0.537
0.078	0.042	0.137	0.538
0.111	0.054	0.176	0.526
0.094	0.048	0.156	0.534
0.104	0.051	0.168	0.527
0.119	0.056	0.184	0.526
0.182	0.078	0.256	0.494
0.231	0.095	0.311	0.467
0.016	0.015	0.050	0.493
0.050	0.031	0.102	0.536
0.089	0.046	0.149	0.540
0.137	0.062	0.203	0.524
0.180	0.077	0.253	0.495

0.230	0.094	0.310	0.468
0.264	0.107	0.350	0.446
0.307	0.123	0.405	0.417
0.347	0.139	0.457	0.393
0.385	0.156	0.511	0.368
0.415	0.169	0.554	0.352
0.447	0.183	0.601	0.336

Table C2 – 2 Full Cycles submerged debris setup tabulated results.

Q [cms]	H [m]	H/P [-]	C_d [-]
0.028	0.023	0.077	0.459
0.034	0.027	0.087	0.457
0.012	0.013	0.044	0.465
0.014	0.016	0.051	0.429
0.010	0.013	0.041	0.429
0.016	0.017	0.054	0.436
0.017	0.017	0.057	0.442
0.019	0.018	0.060	0.446
0.020	0.019	0.062	0.446
0.021	0.020	0.065	0.450
0.022	0.020	0.067	0.448
0.023	0.021	0.068	0.449
0.024	0.021	0.070	0.449
0.025	0.022	0.072	0.447
0.026	0.023	0.074	0.447
0.027	0.023	0.076	0.449
0.028	0.024	0.079	0.442
0.029	0.025	0.080	0.443
0.030	0.025	0.083	0.441
0.031	0.026	0.084	0.445
0.033	0.027	0.087	0.444
0.034	0.027	0.090	0.442
0.036	0.028	0.093	0.436
0.030	0.025	0.083	0.442
0.010	0.013	0.042	0.421
0.082	0.053	0.172	0.398
0.105	0.065	0.212	0.375
0.045	0.035	0.115	0.410
0.072	0.047	0.156	0.408
0.104	0.064	0.210	0.378
0.114	0.069	0.228	0.368
0.126	0.076	0.250	0.354
0.137	0.083	0.272	0.337
0.144	0.087	0.287	0.328
0.157	0.092	0.302	0.330
0.163	0.095	0.313	0.326

0.172	0.101	0.332	0.314
0.179	0.105	0.345	0.308
0.184	0.107	0.351	0.310
0.195	0.113	0.372	0.300
0.206	0.120	0.395	0.290
0.220	0.125	0.410	0.293
0.231	0.138	0.451	0.266
0.088	0.057	0.188	0.378
0.072	0.049	0.161	0.391
0.095	0.061	0.201	0.369
0.066	0.046	0.150	0.398
0.059	0.042	0.137	0.409
0.049	0.035	0.113	0.447
0.052	0.037	0.121	0.432
0.093	0.059	0.193	0.383
0.119	0.071	0.234	0.367
0.129	0.076	0.250	0.360
0.134	0.078	0.257	0.358
0.138	0.081	0.265	0.353
0.150	0.087	0.285	0.344
0.188	0.103	0.338	0.335
0.198	0.108	0.354	0.329
0.165	0.091	0.299	0.354
0.174	0.096	0.314	0.346
0.167	0.092	0.301	0.352
0.158	0.089	0.291	0.353
0.146	0.085	0.278	0.348
0.132	0.078	0.255	0.357
0.123	0.073	0.241	0.363
0.102	0.064	0.209	0.374
0.074	0.050	0.164	0.389
0.163	0.091	0.297	0.351
0.199	0.108	0.355	0.328
0.212	0.115	0.379	0.317
0.234	0.128	0.418	0.302
0.246	0.134	0.440	0.295
0.126	0.075	0.246	0.360
0.023	0.021	0.070	0.445
0.026	0.023	0.075	0.445

0.028	0.024	0.078	0.446
0.030	0.025	0.082	0.439
0.031	0.026	0.085	0.441
0.033	0.027	0.088	0.436
0.034	0.028	0.091	0.436
0.037	0.029	0.096	0.431
0.038	0.030	0.098	0.431
0.040	0.031	0.102	0.431
0.042	0.032	0.105	0.433
0.044	0.033	0.109	0.431
0.048	0.035	0.116	0.425
0.053	0.038	0.125	0.420
0.056	0.040	0.130	0.419
0.060	0.041	0.136	0.416
0.063	0.043	0.141	0.415
0.066	0.045	0.147	0.409
0.070	0.047	0.154	0.407
0.075	0.049	0.162	0.403
0.080	0.052	0.169	0.400
0.090	0.057	0.187	0.388
0.096	0.060	0.198	0.381
0.105	0.066	0.215	0.368
0.147	0.085	0.279	0.347
0.163	0.091	0.300	0.348
0.178	0.098	0.323	0.339
0.195	0.107	0.352	0.326
0.211	0.116	0.381	0.313
0.227	0.126	0.413	0.300
0.255	0.142	0.466	0.280
0.273	0.152	0.498	0.271
0.290	0.162	0.532	0.261
0.312	0.175	0.575	0.250
0.328	0.185	0.606	0.243

Table C3 – 1 Full Cycle submerged debris setup tabulated results.

Q [cms]	H [m]	H/P [-]	C_d [-]
0.011	0.013	0.043	0.411
0.013	0.014	0.047	0.428
0.014	0.015	0.051	0.434
0.016	0.016	0.054	0.450
0.018	0.017	0.056	0.458
0.019	0.018	0.059	0.460
0.020	0.019	0.061	0.465
0.021	0.019	0.064	0.464
0.022	0.020	0.065	0.468
0.024	0.021	0.068	0.467
0.024	0.021	0.069	0.471
0.025	0.022	0.071	0.469
0.026	0.022	0.073	0.468
0.027	0.023	0.074	0.471
0.028	0.023	0.076	0.470
0.029	0.023	0.077	0.475
0.030	0.024	0.078	0.476
0.030	0.024	0.079	0.479
0.032	0.025	0.081	0.477
0.029	0.023	0.077	0.468
0.030	0.024	0.078	0.478
0.030	0.024	0.079	0.479
0.032	0.025	0.081	0.479
0.033	0.025	0.083	0.484
0.024	0.021	0.068	0.480
0.026	0.022	0.072	0.475
0.028	0.023	0.074	0.481
0.029	0.023	0.077	0.477
0.032	0.025	0.081	0.481
0.035	0.026	0.086	0.478
0.037	0.027	0.090	0.483
0.040	0.029	0.094	0.483
0.042	0.030	0.097	0.483
0.044	0.031	0.101	0.483
0.047	0.032	0.104	0.484
0.040	0.029	0.095	0.481

0.045	0.031	0.101	0.487
0.050	0.033	0.108	0.488
0.053	0.034	0.112	0.491
0.057	0.036	0.118	0.492
0.060	0.037	0.123	0.490
0.063	0.039	0.127	0.490
0.066	0.040	0.130	0.492
0.071	0.042	0.138	0.484
0.075	0.044	0.143	0.483
0.078	0.045	0.149	0.478
0.082	0.047	0.153	0.478
0.086	0.048	0.159	0.474
0.090	0.050	0.164	0.475
0.096	0.053	0.173	0.466
0.100	0.055	0.179	0.463
0.104	0.056	0.184	0.459
0.109	0.058	0.191	0.454
0.210	0.098	0.323	0.400
0.104	0.057	0.186	0.456
0.126	0.065	0.215	0.443
0.143	0.072	0.236	0.437
0.155	0.076	0.251	0.432
0.167	0.081	0.264	0.429
0.180	0.086	0.282	0.421
0.190	0.090	0.295	0.414
0.202	0.095	0.312	0.404
0.219	0.103	0.339	0.388
0.226	0.107	0.351	0.381
0.233	0.110	0.362	0.375
0.240	0.114	0.373	0.369
0.252	0.120	0.393	0.358
0.267	0.128	0.419	0.345
0.280	0.134	0.441	0.335
0.294	0.143	0.468	0.321
0.307	0.150	0.493	0.310
0.322	0.159	0.522	0.298
0.332	0.165	0.541	0.291
0.345	0.173	0.567	0.282
0.358	0.181	0.594	0.274

0.367	0.187	0.613	0.267
0.314	0.154	0.506	0.305
0.297	0.144	0.472	0.320
0.252	0.119	0.391	0.360
0.135	0.069	0.225	0.441
0.113	0.060	0.197	0.449

Table C4 – Lake Brazos submerged debris setup tabulated results.

Q [cms]	H [m]	H/P [-]	C_d [-]
0.018	0.017	0.056	0.477
0.015	0.015	0.050	0.477
0.011	0.012	0.041	0.449
0.012	0.013	0.044	0.464
0.014	0.015	0.048	0.473
0.016	0.016	0.051	0.477
0.018	0.017	0.055	0.476
0.020	0.018	0.059	0.480
0.022	0.020	0.064	0.481
0.018	0.017	0.055	0.480
0.021	0.019	0.062	0.485
0.023	0.020	0.066	0.487
0.025	0.021	0.068	0.486
0.027	0.022	0.071	0.487
0.028	0.023	0.074	0.485
0.030	0.023	0.077	0.484
0.031	0.024	0.080	0.483
0.033	0.025	0.083	0.483
0.037	0.028	0.090	0.478
0.040	0.029	0.095	0.476
0.042	0.030	0.098	0.479
0.045	0.031	0.103	0.473
0.047	0.032	0.106	0.477
0.052	0.035	0.115	0.470
0.056	0.037	0.121	0.467
0.060	0.039	0.126	0.464
0.064	0.040	0.133	0.458
0.067	0.042	0.139	0.452
0.072	0.045	0.147	0.449
0.077	0.047	0.153	0.446
0.082	0.050	0.163	0.439
0.088	0.053	0.173	0.430
0.094	0.055	0.181	0.426
0.099	0.058	0.190	0.416
0.103	0.060	0.197	0.411
0.106	0.062	0.204	0.405

0.110	0.064	0.211	0.397
0.102	0.060	0.196	0.410
0.125	0.071	0.234	0.387
0.147	0.082	0.270	0.367
0.115	0.066	0.217	0.396
0.136	0.077	0.254	0.373
0.157	0.088	0.287	0.355
0.166	0.092	0.303	0.349
0.178	0.099	0.324	0.339
0.191	0.105	0.344	0.330
0.199	0.109	0.358	0.325
0.208	0.114	0.373	0.319
0.219	0.119	0.391	0.313
0.229	0.124	0.407	0.308
0.238	0.129	0.422	0.303
0.248	0.134	0.439	0.298
0.267	0.144	0.471	0.288
0.280	0.151	0.494	0.282
0.294	0.157	0.517	0.276
0.310	0.166	0.545	0.269
0.324	0.174	0.570	0.263
0.341	0.182	0.598	0.257

Table C5 – Slope, Full Cycle submerged debris setup tabulated results.

Q [cms]	H [m]	H/P [-]	C_d [-]
0.011	0.013	0.041	0.447
0.014	0.015	0.049	0.456
0.018	0.017	0.056	0.462
0.020	0.019	0.061	0.462
0.022	0.020	0.066	0.466
0.025	0.021	0.070	0.466
0.026	0.022	0.073	0.465
0.028	0.023	0.077	0.462
0.023	0.021	0.069	0.452
0.025	0.022	0.072	0.462
0.027	0.023	0.075	0.463
0.029	0.024	0.078	0.465
0.030	0.024	0.080	0.470
0.028	0.023	0.077	0.466
0.026	0.022	0.072	0.468
0.030	0.024	0.079	0.466
0.031	0.025	0.082	0.466
0.033	0.026	0.085	0.466
0.036	0.027	0.090	0.465
0.038	0.028	0.093	0.463
0.041	0.030	0.098	0.465
0.043	0.031	0.102	0.465
0.045	0.032	0.105	0.462
0.048	0.033	0.109	0.460
0.050	0.035	0.114	0.460
0.054	0.037	0.120	0.457
0.058	0.038	0.125	0.455
0.061	0.040	0.130	0.455
0.064	0.041	0.135	0.452
0.067	0.042	0.139	0.452
0.072	0.045	0.147	0.447
0.076	0.047	0.153	0.443
0.080	0.049	0.159	0.440
0.086	0.051	0.168	0.436
0.091	0.053	0.175	0.431
0.096	0.056	0.184	0.424

0.100	0.058	0.191	0.420
0.104	0.060	0.198	0.413
0.108	0.062	0.202	0.416
0.127	0.070	0.230	0.403
0.137	0.074	0.243	0.400
0.147	0.079	0.258	0.391
0.155	0.083	0.271	0.383
0.117	0.066	0.215	0.410
0.162	0.086	0.283	0.376
0.170	0.090	0.295	0.370
0.178	0.094	0.307	0.365
0.186	0.098	0.320	0.360
0.193	0.101	0.330	0.356
0.202	0.105	0.344	0.350
0.212	0.109	0.357	0.347
0.222	0.113	0.371	0.343
0.230	0.116	0.382	0.340
0.239	0.121	0.396	0.335
0.250	0.126	0.412	0.331
0.266	0.133	0.436	0.322
0.280	0.140	0.460	0.314
0.298	0.149	0.488	0.306
0.317	0.158	0.518	0.297
0.335	0.167	0.547	0.289
0.350	0.175	0.573	0.282
0.364	0.181	0.595	0.277

Table C6 – Slope, Half Cycle submerged debris setup tabulated results.

Q [cms]	H [m]	H/P [-]	C_d [-]
0.011	0.013	0.041	0.449
0.014	0.015	0.049	0.461
0.018	0.017	0.055	0.472
0.019	0.018	0.059	0.474
0.021	0.019	0.063	0.475
0.023	0.020	0.066	0.474
0.024	0.021	0.069	0.475
0.026	0.022	0.071	0.479
0.027	0.022	0.073	0.483
0.028	0.023	0.075	0.484
0.024	0.021	0.068	0.476
0.025	0.021	0.070	0.478
0.027	0.022	0.073	0.475
0.028	0.023	0.075	0.481
0.030	0.024	0.078	0.477
0.031	0.024	0.080	0.478
0.032	0.025	0.082	0.481
0.034	0.026	0.084	0.480
0.037	0.027	0.090	0.480
0.039	0.029	0.094	0.481
0.042	0.030	0.097	0.482
0.044	0.031	0.101	0.482
0.046	0.032	0.104	0.482
0.044	0.030	0.100	0.494
0.048	0.032	0.105	0.494
0.052	0.034	0.111	0.494
0.039	0.028	0.092	0.497
0.035	0.026	0.085	0.489
0.028	0.023	0.075	0.485
0.031	0.024	0.079	0.493
0.037	0.027	0.089	0.489
0.042	0.030	0.097	0.490
0.046	0.031	0.103	0.490
0.028	0.023	0.075	0.482
0.031	0.024	0.080	0.481
0.034	0.026	0.084	0.482

0.040	0.029	0.094	0.482
0.044	0.031	0.101	0.484
0.048	0.033	0.107	0.482
0.052	0.034	0.113	0.483
0.056	0.036	0.118	0.483
0.059	0.037	0.122	0.484
0.063	0.039	0.127	0.482
0.066	0.040	0.132	0.480
0.068	0.041	0.135	0.479
0.076	0.045	0.146	0.476
0.081	0.047	0.154	0.473
0.086	0.049	0.160	0.471
0.090	0.050	0.164	0.470
0.093	0.052	0.170	0.466
0.099	0.054	0.177	0.463
0.103	0.056	0.183	0.460
0.108	0.058	0.190	0.456
0.102	0.055	0.181	0.462
0.124	0.064	0.210	0.452
0.140	0.070	0.230	0.445
0.154	0.076	0.248	0.437
0.167	0.081	0.265	0.429
0.179	0.085	0.279	0.423
0.189	0.089	0.292	0.418
0.200	0.093	0.306	0.414
0.209	0.096	0.315	0.413
0.218	0.099	0.326	0.409
0.231	0.104	0.342	0.404
0.249	0.111	0.364	0.396
0.273	0.122	0.401	0.377
0.262	0.116	0.382	0.388
0.285	0.128	0.420	0.366
0.305	0.137	0.451	0.352
0.322	0.145	0.476	0.342
0.339	0.153	0.502	0.333
0.356	0.162	0.532	0.321
0.375	0.171	0.563	0.311
0.397	0.182	0.596	0.302